Collision Risk-Informed Weather Routing for Sailboats

Marcin Zyczkowski[1*] and Rafal Szlapczynski[1]

[1] Institute of Ocean Engineering and Ship Technology, Gdansk University of Technology, Poland

[*] Corresponding author: e-mail address: marcin.zyczkowski@pg.edu.pl

ABSTRACT

Selected COLREG rules, good seamanship and sheer common sense indicate that it is in a sailboat's interest to follow collision-free routes without relying on large power-driven ships to give way. Until now, however, no method has integrated a sailboat's weather routing with collision risk monitoring and collision avoidance. Therefore, a new deterministic approach to combine the above features within one method is introduced here. The proposed method is based on Dijkstra's algorithm, where edges may be temporarily removed due to the presence of other ships. This paper presents a design of the main weather routing algorithm and the collision risk monitoring part, which applies an elliptic domain generated automatically around the target and dependent on the target's length. The method has been implemented and tested in a series of computer simulations. The results are provided and discussed here. They confirm the method's effectiveness in terms of determining collision-risk-free routes, as well as its acceptable computational time. They also show how the latter can be shortened at the cost of obtaining suboptimal routes. Finally, they emphasize the importance of considering successive weather forecasts, risk monitoring and route updates.

Keywords: sailing vessel, weather routing, collision avoidance, path planning, Dijkstra's algorithm, collision risk

1. INTRODUCTION

According to a recent Annual Overview of Marine Casualties and Incidents by the European Maritime Safety Agency (EMSA) [1] for 2011–2018, sailboats contribute to about 1.5% of all marine incidents. Furthermore, they also contribute to nearly 7% of incidents with very serious casualties. This indicates that, on average, an incident involving a sailing vessel is over four times more likely to result in serious casualties than an incident involving a power-driven vessel. It is also worth noting that about 64% of the serious incidents involving sailboats are attributed to collisions. Thus it is important to monitor and update a sailboat's route to minimize safety threats posed by other ships. As explained below, it is possible and desired from a legal perspective.

Nowadays, knowing the parameters of a sailing vessel, one can use appropriate software (e.g. Bentley Systems package [2]) to obtain the speed characteristics for given wind conditions. When combining this with a digital sea chart and weather forecasts, it is possible to determine a time-minimal route from the starting point to the destination. However, in practice, such a route must be re-planned on the way due to weather forecast updates and unpredicted events, e.g. the proximity of other ships. According to COLREGs, interpreted in [3]: "A power-driven vessel underway shall keep out of the way of a sailing vessel." However, good seamanship requires that sailing vessels avoid approaching other power-driven vessels (particularly when motor-driven ships are moving with constant speed and course). Furthermore, Rule 18 b. states that "A sailing vessel underway shall keep out of the way of: (i) a vessel not under command; (ii) a vessel restricted in her ability to manoeuvre; (iii) a vessel engaged in fishing." According to Rule 13: "any vessel overtaking any

other shall keep out of the way of the vessel being overtaken." And according to Rule 10 (Traffic Separation Schemes): "A vessel of less than 20 metres in length or a sailing vessel shall not impede the safe passage of a power-driven vessel following a traffic lane." Similarly, according to Rule 9 b. (Narrow Channels): "A vessel of less than 20 metres in length or a sailing vessel shall not impede the passage of a vessel which can safely navigate only within a narrow channel or fairway." Clearly, the sailing vessel's priority of way depends on the circumstances, especially in port surroundings, narrow channels or gulfs, where collision risk is above average [4], [5]. Finally, a sailboat may alter her course in advance before a power-driven ship is obliged to give way so as not to count on a manoeuvre of a much larger target.

Until now, there was practically no published research on sailing vessel-dedicated collision risk avoidance. In particular, no works examine sailboat weather routing together with collision avoidance. This paper aims to fill this gap. It proposes a new deterministic route planning method, collision risk monitoring and collision avoidance for a sailing vessel. The method is based on a modified version of Dijkstra's algorithm. This article continues the authors' research on deterministic methods in planning trips for sailing vessels [6], [7]. It focuses on designing and implementing the collision risk avoidance algorithm while outlining a broader route planning method. Apart from the weather routing (WR) and collision avoidance (CA) fusion, the main contributions of the proposed solution compared with other WR methods for sailboats are as follows:

- handling 32 directions of movement on a grid,

- a customized grid resolution (dependent on user preferences),

- taking into account extra time for performing course alteration manoeuvres,

- modelling comfort associated with both navigation and the journey itself by avoiding excessive or too frequent turns (they are penalized in the goal function),

- taking into account weather changes (subsequent weather forecasts are used when planning a route).

All the above features are integrated within a web-based application that implements the presented method. Thanks to them, the application produces routes that address a wide spectrum of navigation needs and preferences, balancing between customized time efficiency and accuracy of modelling and between the route's time and associated comfort.

The rest of the paper is organized as follows. Section 2 presents related works and background. The proposed method's description: an overview is given in Section 3, an environment model in Section 4 and an optimization algorithm with collision avoidance in Section 5. Section 6 contains examples of simulation results accompanied by their discussion. The method's limitations are addressed in Section 7, while Section 8 sums up the paper.

2. RESEARCH BACKGROUND

As this paper combines sailboat weather routing with ship domain-based collision avoidance, these topics are discussed in the respective subsections below.

2.1 Weather Routing

The works on weather routing for sailboats are relatively rare, arguably because most research is done for commercial purposes (regattas) and hence is not published. However, among the existing works, two threads can be distinguished. The first one concerns robotic sailing and covers various

aspects, including route planning [8]. Those works present methods using multiple versions of Dijkstra's algorithm to find the optimal route. Some additionally combine routing with course control [8]. However, only a few of those methods use 32 movement directions on a grid (e.g. [9]), which is essential for achieving higher modelling accuracy.

The second thread includes papers which address the issue of crewed sailboats. Here, some selected aspects of weather routing are also present, although no published method covers its full spectrum. Uncertainty of weather predictions and its impact on decision strategies and tactics was further researched in [10]. The paper proposed a method that, rather than minimising the passage time, aimed at maximising the probability of reaching the destination sooner than the opponent. This topic was continued in [11], which focused on improving the accuracy of weather predictions using an artificial neural network. Both of the above works lead to [12]. The latter documents a dynamic programming-based real-time routing method, which uses weather data and real-time yacht performance. Despite the apparent progress brought by Tagliaferri, it must be noted that none of those three papers integrated the method with Electronic Navigational Charts (ENCs).

A method that overcomes the above limitation of dynamic programming-based solutions was proposed in [13]. It models the environment as a graph and uses Dijkstra's algorithm to find the least-time path, taking into account dynamic weather conditions [14] and map-derived bathymetry-related constraints.

Route planning methods for power-driven ships can be divided into deterministic and non-deterministic. The isochrone method was the first deterministic approach to weather routing; it was designed for manual use and based on geometrically determined and recursively defined time fronts (isochrones). In the following decades, computer implementations of the method were developed. Other deterministic approaches to weather routing for power-driven ships include dynamic programming, A* and related algorithms or graph-based algorithms (Dijkstra's algorithm and its variations). As for dynamic programming, methods for a grid of points have been proposed. Also, 3D dynamic programming approaches to weather routing were applied [15]. Among the Dijkstra-based solutions already mentioned, the VISIR system [16] and method described in [17] are particularly noteworthy. The former uses complex weather modelling, while the latter applies a 3D version of Dijkstra's algorithm with time as the third dimension. Dijkstra's algorithm was also used in [18], where AIS data supported ship weather routing. Other Dijkstra-based methods were presented in [19], but all of them were dedicated to Unmanned Surface Vehicles (USV) rather than conventional power-driven ships. An A* algorithm and its variations were used in [20] and [21], both dedicated to ship routing in ice-covered waters. All the above deterministic methods generally use single-objective optimization, usually focused on minimization of passage time or fuel consumption or aggregating a few objectives into one [17]. A limitation of most deterministic weather routing methods is that they are hardly scalable. For long-distance routing on large maps, it usually means either a rise in the computational time or a decrease in accuracy (if a shorter computational time is needed). This drawback, however, may be overcome in the case of graph-based methods by applying uneven distribution of graph vertices, which can be placed more densely around obstacles and more sparsely on open waters.

Non-deterministic weather routing methods are usually based on meta-heuristics, including genetic algorithms (GAs), evolutionary algorithms (EAs) and swarm optimization, of which ant colony optimization (ACO) is particularly popular. For example, an optimization with Pareto-optimal sets of solutions has been proposed in [22], [23], [24]. In [22], [23], the more robust SPEA/SPEA2, a multi-objective evolutionary approach, has been applied. In [25], while utilising the decision maker's preferences in the same EMO weather routing method has been introduced in [26].

Table 1 A comparison of weather routing methods

Method	Deterministic	Ship type	Optimization method	Other features
[6][7]	Yes	Sailing vessel	Dijkstra's algorithm	Handling wave resistance, ensemble weather forecast, higher modelling accuracy, multi-objective
[8]	Yes	Autonomous sailing vessel	Dijkstra's algorithm	Course control
[9]	Yes	Sailboat	Dijkstra's algorithm	Higher modelling accuracy
[10]	Yes	Sailing vessel	Dynamic programming	Uncertainty of weather predictions
[11]	Yes	Sailing vessel	Dynamic programming	Uncertainty of weather predictions
[12]	Yes	Sailing vessel	Dynamic programming	Uncertainty of weather predictions
[13]	Yes	Sailboat	Dijkstra's algorithm	Dynamic weather conditions, handling wave resistance
[14]	Yes	Sailboat	Dijkstra's algorithm	Dynamic weather conditions, handling wave resistance
[27]	Yes	Sailboat	Dynamic programming	Handling wave resistance
[16]	Yes	Sailboat	Dynamic programming	Uncertainty of weather predictions, wave resistance
[17]	Yes	Sailboat	Dijkstra's algorithm	Multi-objective
[18]	Yes	Sailboat	Dijkstra's algorithm	Based on historical AIS
[19]	Yes	Autonomous sailboat	Dijkstra's algorithm	Energy efficient
[20]	Yes	Autonomous sailboat	A* algorithm	Multi-objective, ice-covered waters
[21]	Yes	Autonomous sailboat	A* algorithm	Multi-objective, ice-covered waters
[22]	No	Sailboat	Multi-objective evolutionary algorithm	Pareto-optimal results
[23]	No	Sailboat	Multi-objective evolutionary algorithm	Handling wave resistance
[24]	Yes	Sailboat	Dijkstra's algorithm, Pareto-optimal, human decision	Ice-covered waters
[25]	No	Sailboat	Multi-objective evolutionary algorithm	Avoiding stability-related phenomena
[26]	No	Sailboat	Multi-objective evolutionary algorithm	Pareto-optimal results

A comparison of weather routing methods is provided in Table 1. All the above methods (deterministic and non-deterministic) are limited in their scope to strict weather routing, not

addressing collision risk monitoring and collision avoidance. Integration of the above two is the main goal of this paper.

2.2 Ship Domain-Based Collision Avoidance

Classifying collision avoidance methods can be done in a number of ways, as evidenced by [28]. Here, the research on ship domain-based collision avoidance systems is divided into two groups, depending on the functional scope of the considered methods.

The first group addresses the trajectory or path planning of a single ship. Considering the proposal's topic, investigating the safety criteria applied by those methods is interesting. In [29], a collision avoidance method based on a genetic algorithm (GA) is presented. The domain is a circle with a radius set arbitrarily to 1.5 NM. The same safety ring is also applied in [30], where a distributed anti-collision system is proposed. [31] presents a method of planning a ship's safe trajectory based on ACO. The method involves a hexagonal domain of a target, though applying other shapes is mentioned. In a later paper [32], the author applies an Artificial Potential Field (APF) approach to the same problem. Again hexagonal ship domain is used. In [33], a more advanced Discrete Artificial Potential Field (DAPF) algorithm was presented, which applied an efficient graph search algorithm for path planning. Determining collision avoidance manoeuvres in harsh weather was researched in [34], and an elliptic domain was used there. A related approach – the velocity obstacle (VO) method – was applied in [35]. GVO can handle multiple targets as moving obstacles in a dynamic maritime environment. Similarly, in [36], a VO algorithm was combined with APF, which enabled USVs to avoid collisions with ships. Another solution for USV was introduced in [37], where the local normal distribution-based trajectory (LNDT) algorithm was applied to determine smooth and COLREG-compliant paths in encounter scenarios, which enables keeping the defined distance from the target ship. A multicriteria collision avoidance method based on expert judgments was presented in [38].

The second group deals specifically with multi-ship encounters. Differential games and artificial neural networks for underwater vehicles – a multi-agent system of controlling a team of homogeneous underwater vehicles was presented in [39], and an iterative model based on an array of discrete transitions between successive states was discussed in [40]. Finally, in [41], apart from a distance at closest point of approach (DCPA), time to closest point of approach (TCPA), relative distance, relative bearing, relative speed and relative heading angle were used for risk assessment leading to the vessel conflict ranking operator (VCRO) developed in [42]. Other collision avoidance-related research includes [43][44], where operations in ice conditions involving multiple vessels are addressed. In general, it might be stated that trajectory-oriented optimization methods from both groups described above stress far-fetched planning [45], and ship domains [46] are either not applied or reduced to basic geometric shapes for computational reasons. A more advanced domain changing dynamically with the operational parameters of a ship was applied in [47].

Until now, practically no papers considered collision risk between sailboats and power-driven ships. However, the accident risk for two or more power-driven ships is well-researched for particular water areas, including river estuaries, harbours [48] and other regions of high traffic intensity [49], [50], [51]. Among others, the collision risk index and related approaches based on analysis of big data and Bayesian networks were introduced in [52][53][54].

Unfortunately, there are no similar systematic works on the probability of sailboat-to-power ship collisions, though the latter is considerable, as evidenced by the EMSA overview [1]. As of now, such solutions have only been developed for autonomous sailboats.

All the weather routing methods in Subsection 2.1 (deterministic and non-deterministic) are limited in their scope to strict weather routing or – generally – to so-called global planning. They do not address the issues of collision risk monitoring and collision avoidance, typically classified as local planning problems. Similarly, collision avoidance methods for sailing vessels from Subsection 2.2 do not integrate their features with weather routing. In the case of sailboats, which depend heavily on wind for their manoeuvring and speed, combining the above features is desired. Namely, a fusion of global and local planning elements is needed. Thus, this paper proposes weather routing extended by early planning of collision avoidance manoeuvres to avoid targets in advance.

3. METHODOLOGY

The proposed route planning method consists of three major steps: reading the input data, transforming them into a graph and finally – determining an optimal route in this graph. The input data include a bitmap of the research area; the number of directions of movement in the graph; grid resolution of the graph; route endpoints; sailing vessel polar diagram characteristics; forecasted wind data and AIS data of a target (a power-driven ship). The latter include the target's length, position, course and speed. Moreover, the following parameters are assumed: light and stable wind, calm water or small waves, full sail setup and all sails reasonably trimmed. To make sure COLREGs are not violated, the sailboat's manoeuvres are performed before the power-driven ship is obliged to give way (the exact time when the manoeuvres start depends on when the algorithm is initiated). However, this does not apply to narrow channels and overtaking, when manoeuvres can be initiated at a reasonably closer distance from a power-driven target.

Based on the above, a directed, time-dependent graph is generated. Following this, a least-time route is determined using an extended heap-based Dijkstra algorithm. The resulting route minimizes total travel time (including the cost of course changes) while avoiding grounding and ship-to-ship collision risk. The main idea behind the method is presented in Figure 1. The speed characteristics of the sailing vessel, included in input data, are obtained by external software in the form of a black box. Subsection 3.2 presents a simplified method of getting them using Bentley MaxSurf VPP.

Transforming the data into a graph is described in Subsection 3.1 while determining a collision-free route is described in Section 4.

Input data

- bitmap of the area
- grid resolution
- sailboat's route start and endpoints
- sailboat's polar diagram characteristics (black box)
- number of directions of sailboat's movement on a grid
- forecasted wind data (grib data)
- length, position, course and speed of a power-driven target ship

↓ **data**

Transformation of the input data to a graph

↓ **a directed time - dependant graph**

Determining an optimal route in a graph

- minimizes total travel time using Dijkstra alghoritm (including the cost of course changes)
- avoids running aground (static bathymetric constraints)
- avoids excessive wind or excessive angle of heel (dynamicweather-derived constraints)
- avoids collision with a target power-driven ship (dynamic constraints)

↓ **result**

Final route recommendation

Figure 1. The method's overview

3.1 Discrete Model of the Environment and Ship's Motion

In this paper, we assume a geographical area limited by parallels and meridians (φ_1, φ_m, λ_1, λ_n). It can take different shapes depending on its exact size and geographical location. For such a limited area, a bitmap can be generated. By taking into account the area's bathymetry, the ship's draught and the necessary clearance under the keel, we can identify navigable and non-navigable points within the area. The total number of all these points depends on the area's size and grid resolution calculated using the following formula:

$$z = \frac{(\varphi_m - \varphi_1)(\lambda_n - \lambda_1)}{d_{lat} d_{lon}} = mn \tag{1}$$

where:

m, n – numbers of horizontal and vertical curves, respectively,
φ_1, λ_1, φ_m, λ_n – minimal and maximal values of the area's geographical coordinates.
d_{lat}, d_{lon} – vertical and horizontal distance between neighbouring points

The described method is based on a discrete model, where the coordinates of each $m \cdot n$ points P_{ij} are:

$$P_{ij} = P(\varphi_i, \lambda_j), \quad i = 1,2,..,m \, ; \, j = 1,2,...,n \tag{2}$$

where:
φ_i – latitude
λ_j – longitude

For each of those points, we store:
- information, whether the point is navigable,
- an array containing forecasted dynamic hydrometeorological conditions changing in time (a sequence of weather forecasts for subsequent timespans).

A particular route segment is navigable if both endpoints are navigable and the segment does not cross non-navigable points. Furthermore, all segments must comply with the assumed discrete directions of the ship's 2D motion.

The number of those directions of movement belongs to the set {8, 16, 32} as shown in Figurere 2.
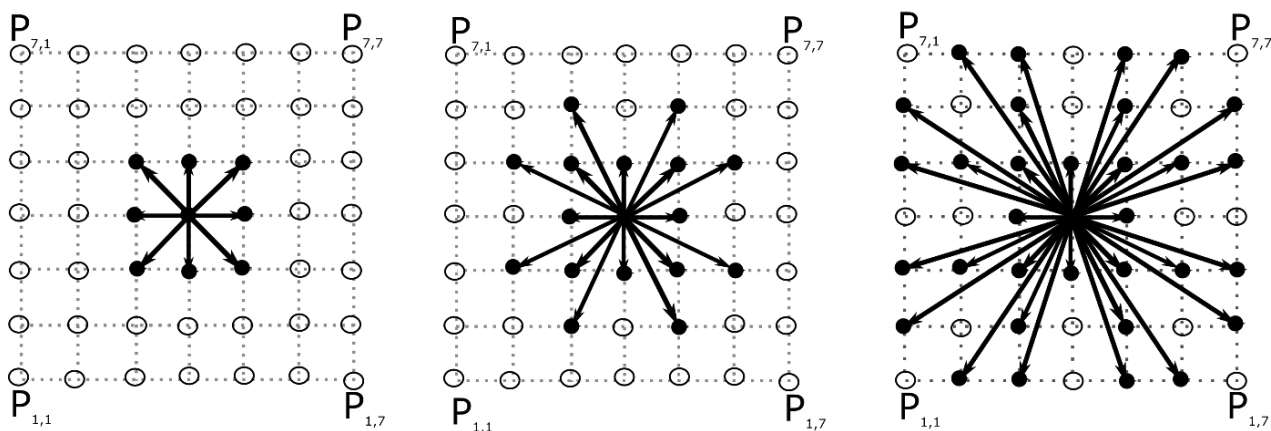

Figure *2*. 8, 16 and 32 directions of movement on a grid

The number of directions depends on the assumed accuracy of route planning: the higher the number of directions, the greater the number of considered routes and the longer the computational time of the method.

Let P_k be a k-th point on a ship's route. Then, knowing the current point P_k in the navigable area, we can consider all possibilities of choosing the next point P_{k+1}, thus forming a new route segment.

An example route from P_1 to P_9 is shown in Figure 3. It consists of eight segments. As shown in Figure 3, the route is as follows: the ship made three manoeuvres changing the course between the starting point and the endpoint (at points P_2, P_4 and P_8). The route is not the shortest one distance-wise but may be the least-time route for some wind conditions.
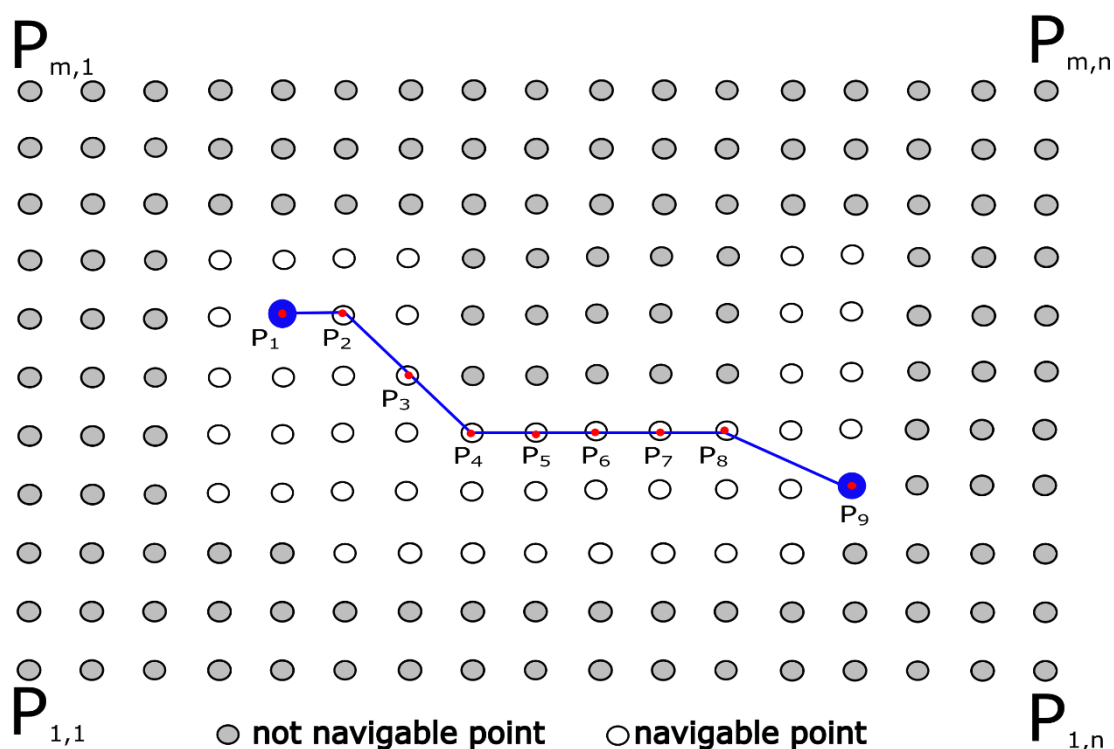

Figure 3. Example route.

The time to get from the current point to the next one is estimated based on the speed characteristics of the sailing vessel. (These characteristics can vary for each ship and are obtained experimentally or estimated by the ship's designers, manufacturers or users.) Knowing hydrometeorological conditions at a given grid point, we can read the sailing vessel's speed from given speed characteristics. The characteristics give the speed as a function of the wind's speed and angle of attack. In this paper, we assume that ship's behaviour depends strictly on the wind and waves [6]. The wave resistance estimation procedure is given in Subsection 4.3.

3.2 Velocity Prediction Program (VPP)

Partly due to sailing ship designers' and classification societies' needs, procedures have been developed to support estimating the basic parameters of a sailing ship's motion. They are referred to as the velocity prediction program (VPP). The relationship between aerodynamics and

hydrodynamics in VPPs is illustrated in Figure 4. Maintaining a balance between hydrodynamics and aerodynamics is required to ensure appropriate VPP parameters. Typically, the estimation of the speed characteristics of a sailing vessel by VPPs is presented for calm water.
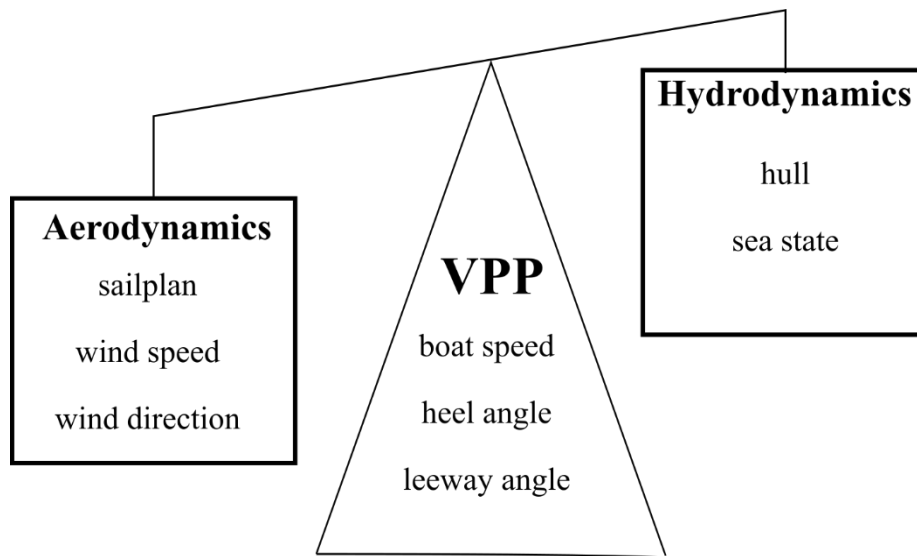

Figure 4. VPP method of speed prediction for a sailing vessel

The result can be presented as a polar diagram of the relationship between the force and direction of the real wind and the speed of the sailing vessel in the selected direction of motion. One of the first methods to estimate speed, roll and drift was proposed in [55]. The iterative procedure to obtain equilibrium sailing conditions was used there to achieve the balance between aerodynamics and hydrodynamics, as shown in Figure 4. To find this balance, one has to solve four nonlinear algebraic equations: hull resistance, hull stability, sail forces and the wind triangle of apparent and true wind velocities and directions. Then, the algorithm iteratively searches for an equilibrium between the known sail driving forces (thrust) and the computed hull resistance corresponding to the sailboat's speed estimated in subsequent iterations.

This paper used the Bentley MaxSurf VPP software (conceptually based on [55]) to estimate the relationship between aerodynamics and hydrodynamics and calculate additional wave resistance.

3.3 VPP and the Procedure for Estimating Wave Resistance

Two dependencies are crucial for determining the speed of a sailing vessel in wavy water. The speed in calm water depends on the speed and relative direction of the wind, and the wave effect that generates the added resistance depends on the speed of the ship and the height and relative direction of the wave.

When the ship sails on a wavy sea, an additional force of added resistance is generated on its hull, this added resistance can be estimated with Bentley MaxSurf. However, it requires providing the sailboat's speed, which also depends on the added resistance. Therefore, an iterative approach was applied to determine the ship's total resistance, similar to [55]. With the sailboat's parameters, the Bentley MaxSurf VPP provides the following output data:
- speed diagram for calm water, which depends on wind speed and angle to the wind,
- hull resistance (R_{hull}) for a given speed (V_s).

The hull resistance (R_{hull}) in MaxSurf VPP is estimated using the Delft II method [56]. The sail generating the effective thrust on calm water ($Thrust_{calm}$) approximated using a meta-model in

Formula (4) is equivalent to hull resistance (R_{hull}), where the effective sail thrust is the thrust considering the losses resulting from sail/hull interaction.

Based on the results produced by Maxsurf VPP, the diagram of vessel speed (V_s) is approximated by a meta-model (a fifth-order polynomial), which takes into account wind speed (V_w) and wind direction angle (β_{TW}):

$$V_s = \sum_{i=1}^{5} p_i V_w^i \beta_{TW}^{5-i}, \qquad (3)$$

where:
p_i – polynomial coefficients

The hull's resistance in calm water is also approximated by a meta-model (a fifth-order polynomial). We assume that this resistance equals the effective sail thrust (Thrust$_{calm)}$.

$$Thrust_{calm} = \sum_{i=1}^{5} p_i V_s^i \qquad (4)$$

We assess the added hull resistance to waves by applying a method based on the strip theory described in [57] and applied in MaxSurf Motion. We assume that the total hull resistance is given as:

$$R_T = R_{hull} + \Delta R \qquad (5)$$

The additional resistance ΔR produced by MaxSurf Motion is also approximated by a meta-model (this time a third-order polynomial).

$$\Delta R = \sum_{i=1}^{3} p_i V_w^i \beta_{TW}^{3-i} \qquad (6)$$

Following this, the balance of forces is assessed, and the effective sail thrust (*Thrust$_{corr}$*) is computed:

$$Trust_{corr} = Trust_{calm} - \Delta R \qquad (7)$$

Then, for the corrected sail thrust (*Thrust$_{corr}$*), the new vessel speed (V_{scorr}) is read from the initial VPP. Their relation can be described by:

$$V_{scorr} = \frac{\sum_{i=0}^{3} p_{i+1} Thrust_{corr}^i}{\sum_{i=0}^{3} q_{i+1} Thrust_{corr}^i} \qquad (8)$$

Finally, the added resistance (ΔR_{corr}) is re-assessed for the updated speed (V_{scorr}). Then, the sail thrust (*Thrust$_{calm}$*) is reduced by the new added resistance (ΔR_{corr}), and the updated speed (V_{scorr}) is calculated again. The above procedure is repeated iteratively until thrust and resistance balance each other, and there is no significant change in the updated speed (V_{scorr}) in the last iteration. This way, the procedure produces the result – the sailboat's speed, including wave resistance.

3.4 Ship's Speed and Passage Time

We assume that the wind vector ($\overrightarrow{W_k}$) is constant for a given weather forecast.

$$\vec{W}_k = (w_k, \beta_k) \tag{9}$$

where:
w_k – wind's true speed at point P_k
β_k – wind's true direction at point P_k

The speed of the ship between points P_k and P_{k+1} is thus estimated according to the formula:

$$V(P_k, P_{k+1}) = v(\vec{W}_k, \alpha_{k,k+1}) = v(w_k, \beta_{k,k+1}) \tag{10}$$

where:
$\alpha_{k,k+1}$ – sailing vessel's course (direction of movement) between point P_k and point P_{k+1}, $\alpha_{k,k+1} = 0°$ for the north direction.
$\beta_{k,k+1}$ – wind attack angle on the ship moving between P_k and P_{k+1}
$v(w_k, \beta_{k,k+1})$ – vessel's speed calculated based on polar diagram characteristics for a given wind speed w_k and direction $\beta_{k,k+1}$.

Segment length from point P_k to point P_{k+1} is the distance between these nodes based on their geographical coordinates.

$$d(P_k, P_{k+1}) = \sqrt{\begin{array}{c}(\varphi_k - \varphi_{k+1})^2 + \\ ((\lambda_k - \lambda_{k+1}) \cdot cos((\varphi_k + \varphi_{k+1})/2))^2\end{array}} \tag{11}$$

The passage time of a segment is denoted by $t(P_k, P_{k+1})$ and calculated using the formula:

$$t(P_k, P_{k+1}) = \frac{d(P_k P_{k+1})}{V(P_k, P_{k+1})} \tag{12}$$

3.5 Optimization Objective

For each route segment, its passage time is a quotient of the distance and the ship's speed. The total time spent on the route is a sum of segments' passage times. However, the objective function also includes time-equivalent penalties for course changes between segments.

$$f = \sum_{k=1}^{n-1} t(P_k, P_{k+1}) + \sum_{k=2}^{n-1} z(P_{k-1}, P_{k+1}), \tag{13}$$

where:
n – the number of route vertices,

$t(P_k, P_{k+1})$ – the ship's passage time from P_k to P_{k+1},

$z(P_{k-1}, P_{k+1})$ – a function that returns a penalty for manoeuvres according to Formula (14). Due to this penalty, manoeuvres are kept to a minimum and only made when needed for collision avoidance or when they result in taking advantage of wind and gaining speed. The penalty can be configured by means of setting a time-equivalent delay ($t_{\Delta\alpha}$). This delay does not affect the route's physical time (which is computed by the first part of Formula (13)) but only the objective function value.

This way, it is possible to balance the route's total time and comfort of navigation (avoiding too frequent or too large turns).

$$z(P_{k-1}, P_{k+1}) = \mid \propto_{k-1,k} - \propto_{k,k+1} \mid \cdot t_{\Delta\alpha}, \tag{14}$$

where:

$\propto_{k-1,k}$ – course over ground from P_{k-1} to P_k,

$\propto_{k,k+1}$ – course over ground from P_k to P_{k+1},

$t_{\Delta\alpha}$ – the time-equivalent penalty delay for a given course change expressed in seconds per degree. It may be configured by the user, and the default value is given in Table 5 (Section 6). The default value is set based on consideration of the data presented in [12]. It must be mentioned here that it does not have to be the actual time of manoeuvring, and this parameter is not used for modelling the sailboat's motion. On the contrary – it is purposely higher to avoid unnecessary turns and determine smoother routes. The minimal course change penalized by the function described in Formula (14) is 11.25 degrees, which results from handling 32 movement directions.

As for optimization constraints, they are as follows:
- static map-derived bathymetric constraints (not navigable cells),
- dynamic collision risk constraints (the sailboat must avoid violating a power-driven vessel's domains).

Finding the shortest route according to the objective function (13) while meeting the constraints is done by means of Dijkstra's algorithm described in Section 5. The algorithm considers turn penalties and graph edges, whose weights change in time due to using subsequent wind forecasts.

4. ROUTE PLANNING AND AVOIDING COLLISIONS WITH POWER-DRIVEN SHIPS

The main routing algorithm with collision avoidance is given in Figure 5. It applies a heap-based version of Dijkstra's algorithm significantly faster than a standard one. The algorithm operates on a time-dependent graph whose edges' weights are determined using weather forecasts.

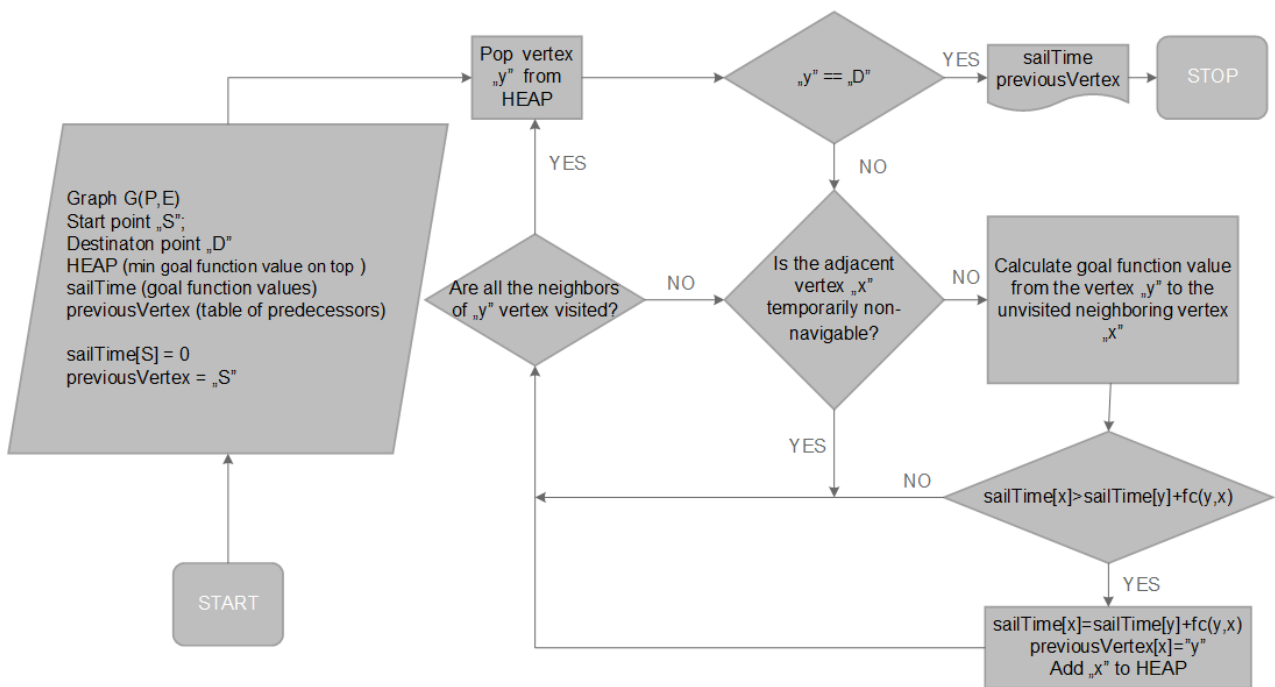**Collision avoidance for Dijkstra algoritm**

Figure 5. Route planning main algorithm, including collision avoidance

The collision avoidance sub-algorithm, which uses the concept of a ship domain, is depicted in Figure 6. Its elements are described in more detail in the following subsections. Due to the apparent uncertainties related to targets' courses and speeds, the algorithm is re-run for the currently available data if any change in targets' courses or speeds is detected.

4.1 A Power-Driven Ship's Domain Modelled on the Grid

When considering a power-driven ship, some points become temporarily non-navigable. We assume that a power-driven ship moves at a constant speed and course. Based on the ship's length, a safety domain is generated around her, which moves with the ship's speed. From a collision avoidance point of view, the ship's domains should be asymmetric (starboard sector wider than port sector) as observed in [58], [59] to favour manoeuvres to starboard in case of head-on encounters (as dictated by COLREGs). However, a sailing vessel's evasive manoeuvres are not regulated by COLREGs. In practice, they are strongly dependent on the wind direction. Therefore, a symmetric elliptic domain is used in this research, and its shape is based on the empirical domains. Based on the ship's length (L), the dimensions of the elliptic domain are as depicted in Figure 6:

- $a = 8L$ (a semi-major axis),
- $b = 4L$ (a semi-minor axis),
- $\Delta a = 4L$ (a ship's offset from the ellipse's centre towards the aft, along the semi-major axis).
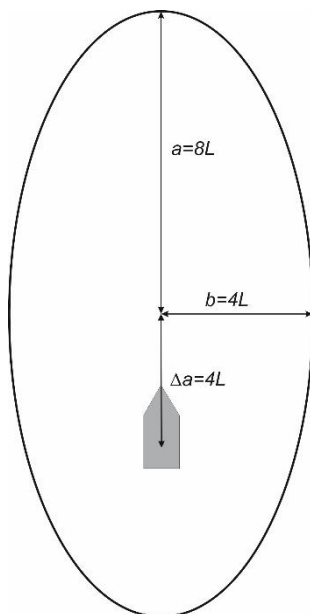
Figure 6. Target ship domain dimensions, where L is the target's length.

Based on the above, a degree of domain violation (DDV) described in detail in [60] is used to establish the ship collision risk. DDV is a parameter with a 0–1 range, where 0 means no collision risk (target ship domain violation) is predicted, while values approaching 1 indicate increasing domain violation (translating to a rise in collision risk) up to the point of two ships' centres overlapping with a DDV of 1. For an encounter with a target, the DDV is defined as:

$$DDV = \max(1 - f_{min}, 0), \tag{15}$$

where f_{min} is the scale factor by which the target's domain has to be multiplied so that the own ship passes on the boundary of the f_{min}-scaled target's domain. When the f_{min} is 1, it means that the own ship will touch the target domain's boundary. While the f_{min} smaller than 1 represents predicted domain violations, values larger than 1 mean that the domain will not be violated throughout the encounter. An example is shown in Figure 7. The target's current position in the own ship's relative coordinate system is shown in the right part. As the target moves in this relative coordinate system, it will reach the position on the left, about 1 NM from the own ship. As can be seen, the own ship will then violate the target's domain (external ellipse) by passing on the boundary of the internal ellipse, whose dimensions are 0.5 times those of the external one. Hence the f_{min} is 0.5, and the DDV is equal to $1 - f_{min}$, which is also 0.5.
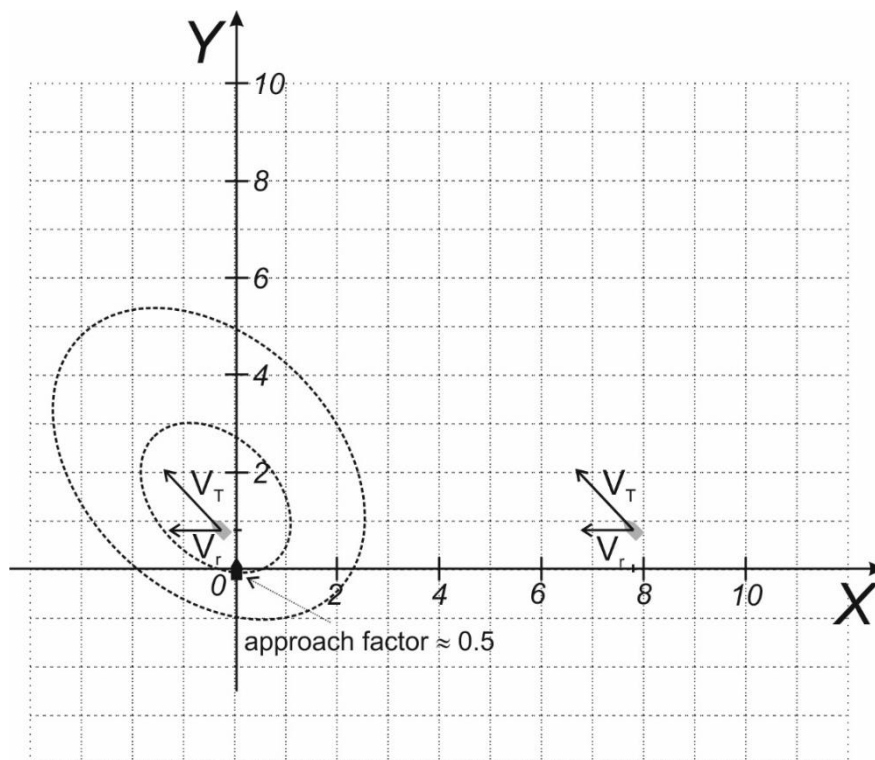
Figure 7. A predicted violation of the target's domain in the own ship's relative coordinate system. The target's current position is shown on the right, and the target's predicted relative position is shown on the left.

4.2 Determining Grid Points within the Domain's Boundary

As the vessel and the domain move, the temporarily non-navigable points within the domain's boundary also change. Below, we describe the procedure for checking whether point $P_{i,j}$ is within the domain boundary at time t. If so, then $P_{i,j}$ is temporarily non-navigable.

Target ship parameters:

- L – length [NM],
- α – true course [deg.], measured clockwise from the north.
- φ_t – latitude coordinate of the current true geographical position [deg.],
- λ_t – longitude coordinate of the current true geographical position [deg.],

Map parameters:

- d_{lat} – latitudinal size of a grid cell (a latitudinal distance between two neighbouring grid points) [NM],
- d_{lon} – longitudinal size of a grid cell (a longitudinal distance between two neighbouring grid points) [NM].

The procedure is based on checking whether a given point of the sailboat's route lies within an ellipse enclosing the target ship's current position. First, the target's true coordinates φ_t and λ_t are converted to virtual coordinates $(x_T, y_T) = (0,0)$ – the target's position becomes a "zero" point of the virtual coordinate system. Then, the sailing vessel's potential position on grid $P_{i,j}$ is converted to

virtual coordinates (x_S, y_S), which denote the distances in nautical miles from the "zero" point (the target's position). An example of the sailboat and target's domain in the virtual coordinate system is shown in Figure 8.
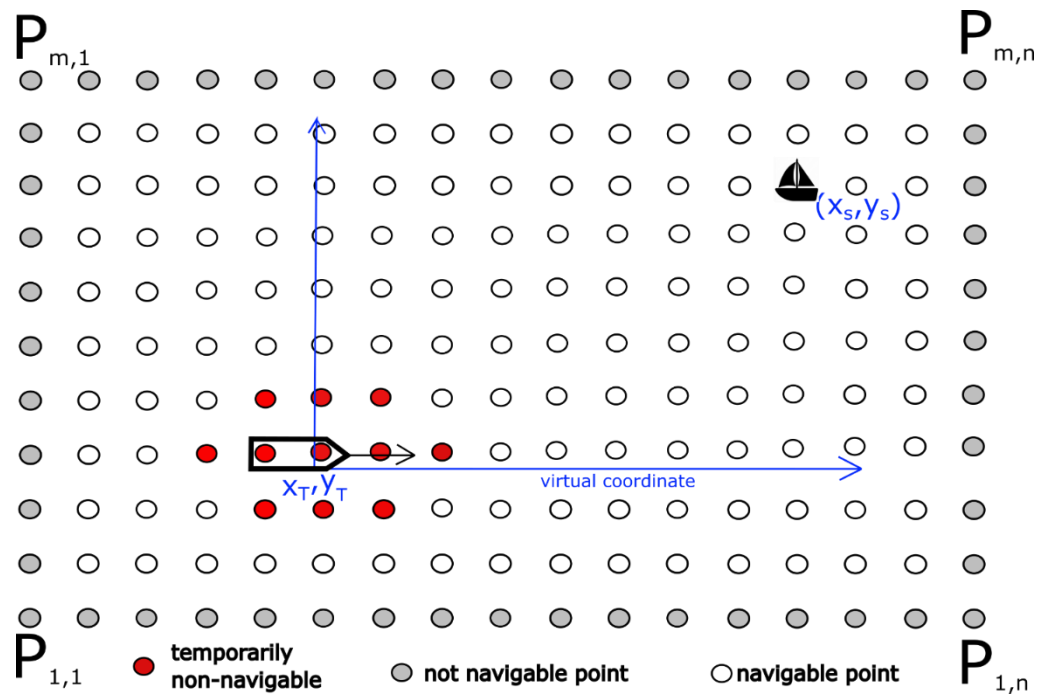
Figure 8. Sailing vessel and target's domain in the virtual coordinate system.

Relative coordinates of the target ship's rotated ellipse's centre (x_e, y_e) with regard to the checked point (x_S, y_S) are:

$$X_e = x_T + \Delta a \cos\alpha - x_S, \tag{16}$$

$$Y_e = y_T + \Delta a \sin\alpha - y_S. \tag{17}$$

Since virtual coordinates (x_S, y_S) were obtained by conversion from grid coordinates of the potential sailboat position $P_{i,j}$, their accuracy is limited by predefined latitudinal and longitudinal grid cell sizes d_{lat} and d_{lon}. To compensate for the error of the grid accuracy, Formulas (16) and (17) have to be supplemented by additional elements $\frac{d_{lat}}{2}$ and $\frac{d_{lon}}{2}$:

$$X_0 = X_e \pm \frac{d_{lon}}{2}, \tag{18}$$

$$Y_0 = Y_e \pm \frac{d_{lat}}{2}, \tag{19}$$

Thus, the grid point will be within the target's elliptical domain if

$$\frac{(X_0 \cos\alpha + Y_0 \sin\alpha)^2}{a^2} + \frac{(X_0 \sin\alpha - Y_0 \cos\alpha)^2}{b^2} \leq 1, \tag{20}$$

If (20) is satisfied for any of the combinations of X_0, Y_0 given by (18–19 the sailboat would violate the target ship's domain if it occupied grid point $P_{i,j}$ simultaneously with the target ship's position being (ϕ_t, λ_t). Thus, the grid point $P_{i,j}$ needs to be marked as temporarily non-navigable.

An example of the vessel's domain and the temporarily non-navigable points is shown in Figure 9.
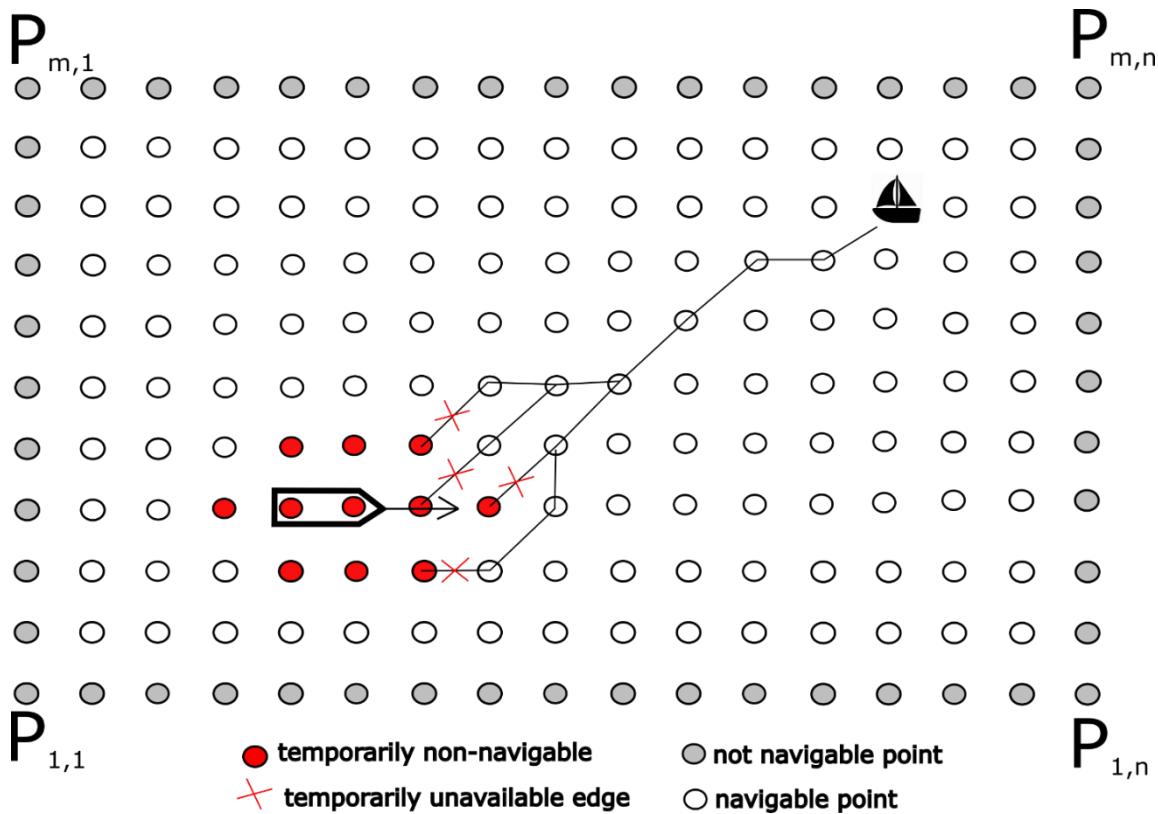

Figure 9. New points as temporarily non-navigable points.

5. VERIFICATION AND SIMULATION DESCRIPTION

The described route planning method was implemented as simulation software for carrying out simulation tests. The following simulations were carried out:

- verification of the method's safe and COLREG-compliant results based on 23 basic scenarios that include various courses and bearings of an engine vessel (Subsection 6.1),
- illustration of the method's performance based on four detailed scenarios that cover various encounters (Subsections 6.2),
- the method's sensitivity study and a brief analysis of how the ship domain modelling affects computational time (Subsection 6.3),
- an example of how the method benefits from taking into account subsequent weather forecasts (dynamic data) in advance during route planning (Subsection 6.4),
- an example illustrating the method's risk monitoring module and route update due to a change in the power-driven ship's course or speed (Subsection 6.5).

Unfortunately, it was impossible to compare our method results with other methods, as there are no such methods with a comparable functional scope (direct fusion of weather routing and early collision avoidance). However, the unique features of the proposed method are discussed in Section 3.

All tests were carried out on a PC: Intel Xeon E3-1270 v6 3.8 GHz, 32 GB RAM. The computational time to find the route depends on the number of graph vertices and movement directions. Table 2 provides computational times for various values of the two parameters mentioned above.

Table 2 The method's computational times depending on the number of graph vertices and movement directions. The route's approx. length is 200 NM

Number of vertices	Movement directions	Computational time [min]
145,231,21	32	< 70
145,231,21	8	< 30
363,276,1	32	< 25
363,276,1	16	< 10
363,276,1	8	< 6
909,181	32	< 6
227,791	32	< 2

5.1 Configuration Data

The tests were carried out on a CONRAD 1200 RT sailing vessel, whose speed characteristic is shown in Figure 10 and Table 3. The speed characteristic is for a sailboat in full sail. Parameters of this sailing vessel and power-driven vessel are given in Tables 4 and 5, respectively. The data from Table 5 were used to generate the target ship's safety domain.
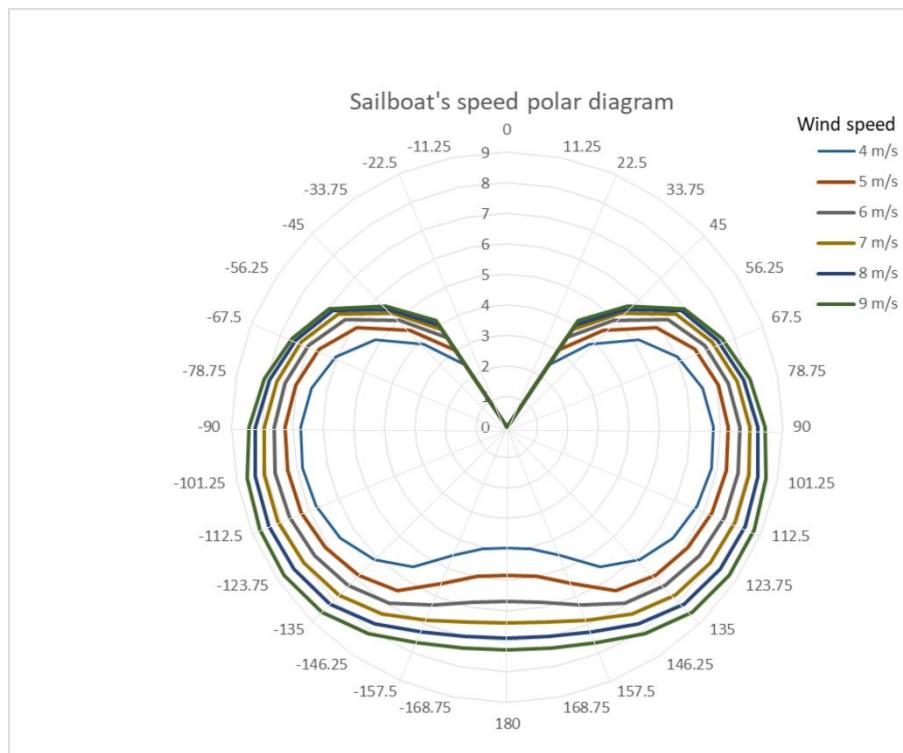
Figure 10. Sailboat's speed polar diagram for full sail and the wind from the 0 degrees direction.

Table 3. Polar diagram of the sailing vessel Conrad (knots).

Wind speed [m/s]	0	11.25	22.5	33.75	45	56.25	67.5	78.75	90	101.25	112.5	123.75	135	146.25	157.5	168.75	180
4	0	0	0	2.46	3.82	5.17	6.05	6.52	6.75	6.81	6.74	6.53	6.13	5.49	4.54	4.07	3.95
5	0	0	0	3.04	4.46	5.88	6.64	7.04	7.24	7.31	7.27	7.12	6.85	6.42	5.54	4.99	4.84
6	0	0	0	3.53	4.93	6.34	7.01	7.39	7.61	7.71	7.70	7.57	7.34	6.94	6.31	5.86	5.71
7	0	0	0	3.86	5.25	6.64	7.27	7.67	7.94	8.07	8.09	7.99	7.77	7.36	6.84	6.52	6.41
8	0	0	0	4.03	5.44	6.85	7.46	7.90	8.21	8.37	8.43	8.37	8.18	7.76	7.27	6.99	6.91
9	0	0	0	4.19	5.59	6.98	7.60	8.09	8.43	8.65	8.75	8.74	8.56	8.13	7.63	7.36	7.30

Table 4. CONRAD 1200 RT – sailing vessel details

Parameter	Value	Units
Volume (displaced)	8.45	m^3
Draught amidships	2.00	m
Length overall	12.00	m
Beam max	4.04	m
Sail area	80	m^2

Table 5. Target ship's parameters and target's domain

Parameter	Value	Units
Target ship's length (L)	300	m
Latitudinal size of a map cell (d_{lat})	0.17	NM
Longitudinal size of a map cell (d_{lon})	0.09	NM
Semi-major axis of an elliptical domain (a)	1200 0.65	m NM
Semi-minor axis of an elliptical domain (b)	600 0.32	m NM
Target's offset from the ellipse's centre towards aft (Δa)	300 0.16	m NM

5.2 Verification – Basic Scenarios

A set of 23 scenarios were designed to verify the method. The main purpose of those tests was to check whether the determined manoeuvres were safe in collision avoidance. It was assumed that a correct path of the sailboat should always avoid violating a power-driven vessel's domain, and additionally, for crossing and head-on encounters, the sailboat should fulfil the following conditions:

a) turn to starboard unless such a turn could lead to a collision course with the target also turning to starboard (target on starboard traverse or behind starboard traverse),
b) pass astern of the target unless it could lead to a collision course with the target turning to starboard,
c) in case of passing ahead of the target, keep a large (predefined) distance from the power-driven ship's bow.

Since verification is limited to computer simulations, it does not cover weather forecast-related uncertainties and modelling inaccuracies. However, the method's sensitivity to both issues is investigated separately in Subsection 6.3

The scenario data are given below. Figure 11 provides the data for all 23 verification cases. They cover only head-on and crossing encounters with a power-driven vessel. As a slower vessel, the sailboat cannot overtake a power-driven ship. And a sailboat overtaken by a power-driven ship should not manoeuvre. Therefore, such cases are not included here. As for the data shown in Figure 11, the wind and the sailboat's initial course and speed are the same for all cases, while the power-driven vessel's course and bearing changes. The initial distances between the two ships are such that TCPA would be 45 minutes for each case.
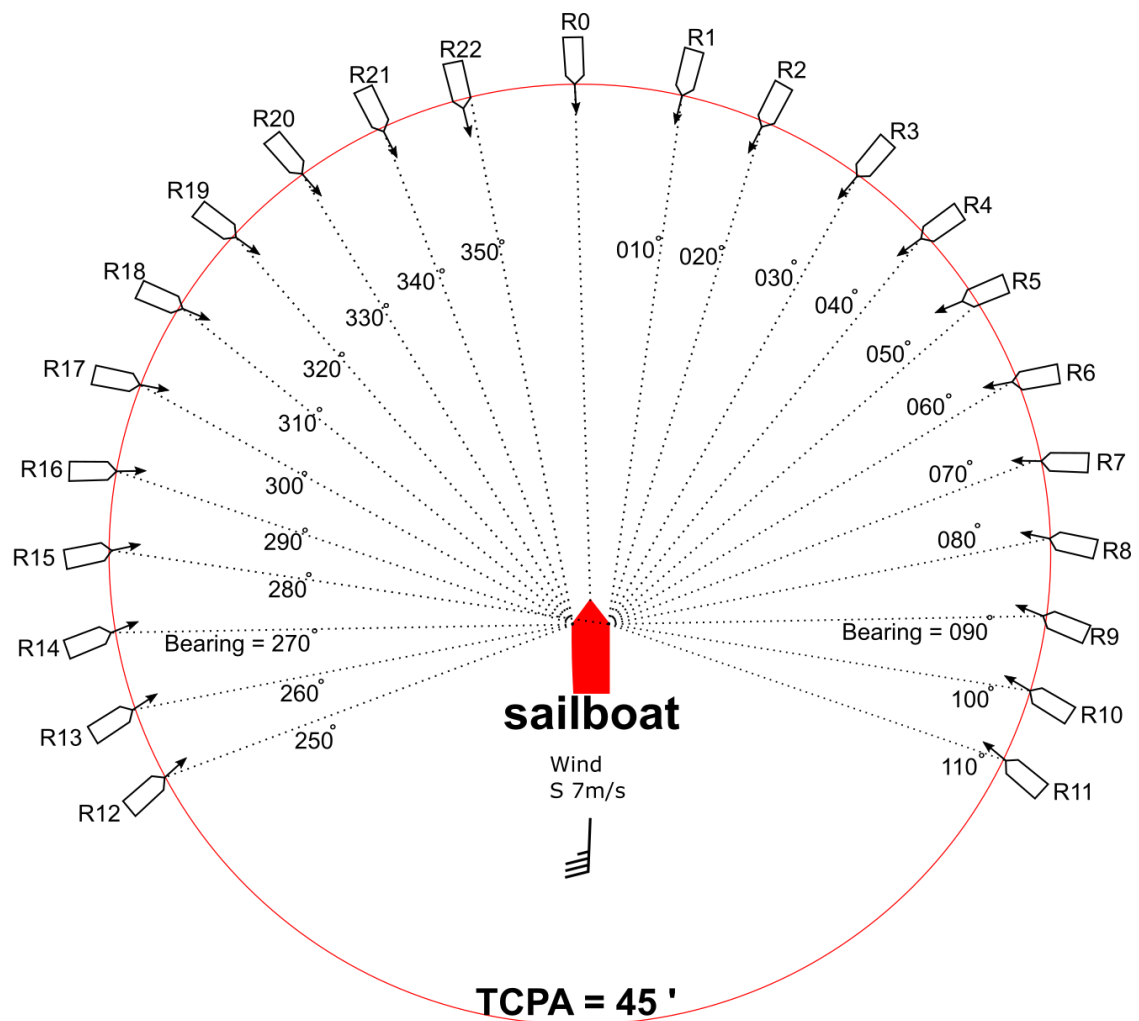
Figure 11. Verification test cases: 23 bearings from power-driven vessel to sailing vessel

5.3 Detailed Scenarios

Additionally, four detailed scenarios were designed to illustrate the results. The data are provided in Table 6. In each scenario, a target travels at a constant course and speed. The wind's direction and speed are read from two subsequent forecasts. It is assumed that a forecast is valid for 5 hours and then replaced with a subsequent one (except for scenario 4, where it is almost 7 hours). The wind change may not directly affect the sailboat's evasive manoeuvres. However, knowing the second forecast in advance makes it possible to plan a more time-efficient route. Without those data, the whole route would be planned differently, resulting in a longer total time.

As for the last parameter in Table 6, it is not the actual time of manoeuvring and is not used for motion modelling. It is a purposely higher value for the optimization method to penalize frequent or excessive turns and thus determine smoother routes.

Table 6. Simulation scenarios

	Scenario 1	Scenario 2	Scenario 3	Scenario 4
Sailing vessel start position	54.81° N 17.37° E	54.47° N 18.85° E	54.95° N 19.67° E	55.38° N 17.87° E
Sailing vessel destination position	55.67° N 18.37° E	54.84° N 19.43° E	55.06° N 18.08° E	55.58° N 17.87° E
Target ship start position	55.24° N 17.87° E	54.69 ° N 19.73 ° E	55.00° N 19.14° E	55.56° N 17.87° E
Target ship speed and course	5 kt 180°	5 kt 270°	5 kt 270°	5 kt 180°
Distance and bearing at the start	40 NM 125°	33 NM 065°	19 NM 280°	50 NM 090°
Sailboat initial relative position xs, ys	-88 -106	-158 -40	96 -9	-261 0
Wind speed and direction	N 7 m/s (<300 min) and SE 7 m/s(> 300 min)	N 7 m/s (<300 min) and E 7 m/s(> 300 min)	S 7 m/s (<300 min) and SW 7 m/s (> 300 min)	N 7 m/s (<300 min) and E 7 m/s (> 400 min)
$t_{\Delta\alpha}$ factor used in Formula (14)	8 s / deg.			

6. PRESENTATION OF THE RESULTS

This section presents the results: the outcome of the main verification is provided first (Subsection 6.1), followed by the detailed simulation results (Subsection 6.2).

6.1 Verification Results

The results for those 23 verification cases are given in Table 7.

Table 7. Results of verification test cases

Sailboat: course 0°, speed 5.7 kt; Wind: 7m/s S; Power-driven target's speed: 15 kt; TCPA: 45 min						
Case	Initial bearing [°]	Initial distance [NM]	Target's course [°]	DCPA [NM]	Sailboat's manoeuvre	Passing astern / ahead of target
R0	0	15.5	180	2.6	To starboard	15.5 NM, N/A

R1	10	15.4	194	2.5	To starboard	35.0 NM astern
R2	20	15.3	207	2.7	To starboard	15.7 NM astern
R3	30	14.6	220	2.9	To starboard	13.2 NM astern
R4	40	14.3	234	3.5	To starboard	14.4 NM astern
R5	50	13.2	247	3.2	To starboard	8.7 NM astern
R6	60	13	259	4.8	To starboard	9.0 NM astern
R7	70	12.4	271	4.0	To starboard	9.0 NM astern
R8	80	11.3	282	3.9	To starboard	10.0 NM astern
R9	90	10	292	3.7	To port	10.0 NM astern
R10	100	9.6	302	3.2	To port	9.0 NM astern
R11	110	9	311	3.2	To port	9.0 NM astern
R12	250	9	49	3.1	To starboard	8.0 NM astern
R13	260	9.6	58	2.5	To starboard	7.0 NM astern
R14	270	10.4	68	2.4	To starboard	6.5 NM astern
R15	280	11.2	78	2.6	To starboard	7.3 NM astern
R16	290	12	89	2.6	To starboard	7.3 NM astern
R17	300	12.8	101	3.1	To starboard	6.9 NM astern
R18	310	13.5	113	4.1	To starboard	6.2 NM ahead
R19	320	14.2	126	3.1	To starboard	6.8 NM ahead
R20	330	14.7	139	2.6	To starboard	8.7 NM ahead
R21	340	15.2	153	2.7	To starboard	8.9 NM ahead

| R22 | 350 | 15.4 | 166 | 2.6 | To starboard | 10.9 NM ahead |

For the majority of the test cases, the sailboat turns to starboard and passes astern of the power-driven target. In cases R9 to R11, the target is starboard traverse or slightly behind starboard traverse. It is impossible then to combine turning to starboard with passing astern of the target. Furthermore, if both ships turned to starboard, it could lead to a collision because the two simultaneous manoeuvres could cancel each other's effect. Therefore turning to port and passing astern of the target is the correct solution. As for cases R18 to R22, the sailboat initially has the target on port, so turning to starboard leads automatically to crossing ahead. The manoeuvre is performed at a large distance, and later the sailboat passes astern of the target when getting back to the initial course. The only alternative to crossing ahead would be turning to port. This could result in a collision if the target turned to starboard (again – the two manoeuvres could cancel each other's effect). So a turn to starboard performed by the sailboat was the correct solution. Finally, in R0, the sailboat is ahead of the target's beam at the start and instantly turns to starboard. This solution is also correct, although it cannot be classified as either crossing ahead or passing astern (hence "not applicable" in the first row).

6.2 Simulation Results

Numerical test results are given in Table 8, followed by their illustration in Figures 12 to 15. Furthermore, DDV [60], introduced in Subsection 4.1, is used for monitoring ship collision risk development along the minimum-time route of each scenario.

Table 8. Simulation results

	Scenario 1		Scenario 2		Scenario 3		Scenario 4	
Collision avoidance mode turned on	NO	YES	NO	YES	NO	YES	NO	YES
Number of course changes	3	4	4	5	1	2	1	8
Total time	588'	617'	340'	349'	450'	456'	595'	598'
Extra time spent on evasive manoeuvres	N/A	+ 29'	N/A	+ 9'	N/A	+ 6'	N/A	+ 3'
Potential collision time (for collision avoidance mode turned off)	189'		216'		393'		238'	
Distance and bearing at collision time	6 NM, 090°		2.9 NM, 290°		3.8 NM, 195°		3.8 NM, 010°	
Parallel distance related to the power-driven ship's velocity vector at collision time	0 NM		2.7 NM		0 NM		0 NM	
Perpendicular distance related to the power-	6 NM		1.1 NM		3,5 NM		3.5 NM	

driven ship's velocity vector at collision time				

In **Scenario 1,** a sailing vessel avoided collision with a power-driven target on her port. As shown in Figure 12, the minimum-time route (marked as a dotted blue line) without considering collision risk would result in a close-quarters situation and possible incident. The collision risk for this minimum-time route is shown in Table 9. The target's domain would be violated about 185 minutes from the simulation start, and DDV would rise to 0.8 after the subsequent 4 minutes, meaning a significant risk of a physical incident. In contrast, the updated route (marked as a solid blue line) avoids this collision risk – DDV remains 0 along the route. The sailing vessel tacks strongly to her port and passes astern of the target at a distance of 6 NM. The target's domain is not violated, as its astern sector's length is about 0.65 NM. Avoiding collision is done at the cost of about 29 minutes (5% of total passage time).
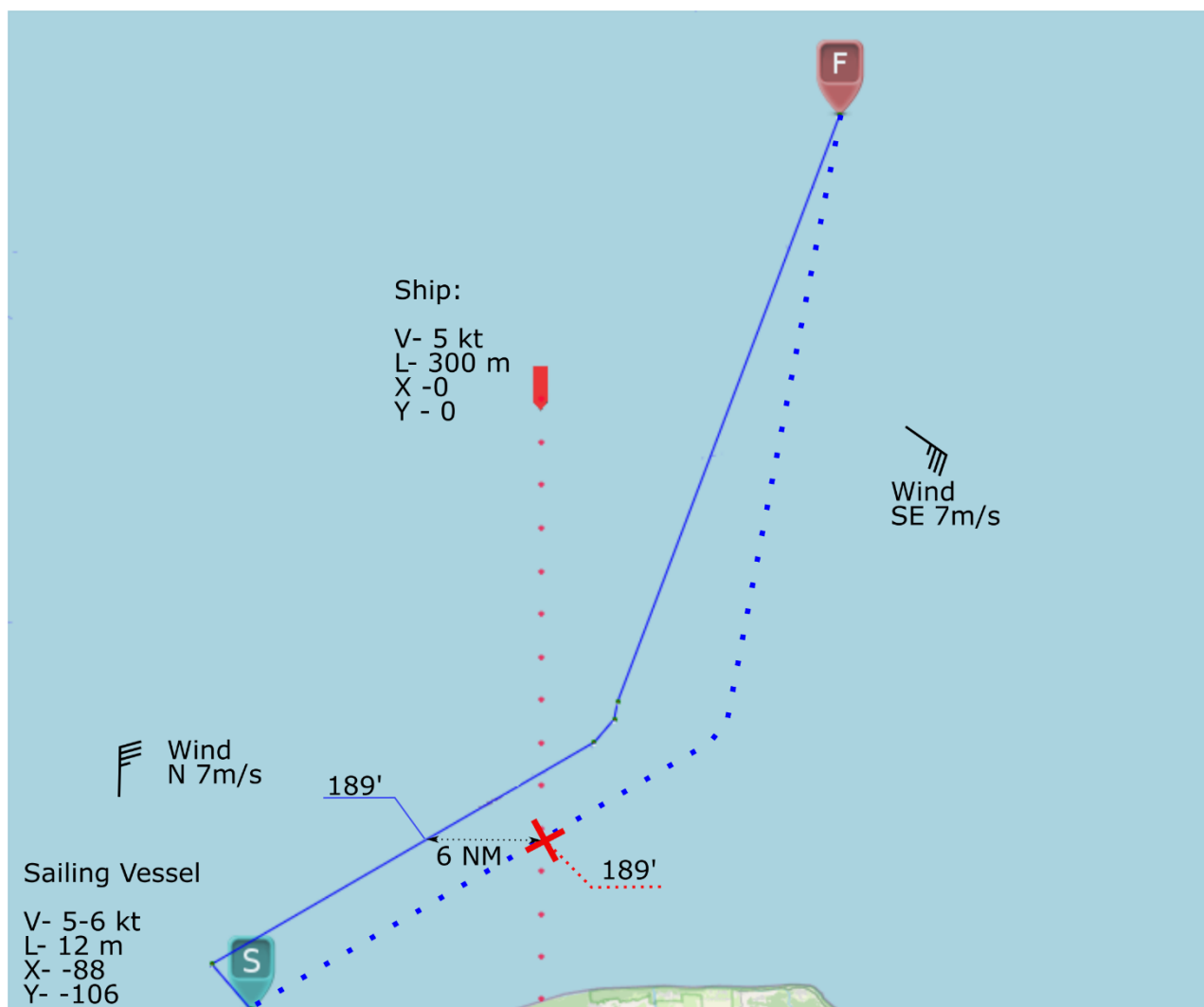

Figure 12. Scenario 1: A sailing vessel avoids collision with a power-driven ship by passing astern, which requires a substantial turn to port. Least-time route of a sailing vessel is marked as a dotted blue line, collision avoidance route – as a solid blue line and the target's path – as a dotted red line.

Table 9. Collision risk for Scenario 1 (minimum-time route marked as the dotted blue line in Figure 12).

Time [min]	183	189	195	201	208	214
DDV [/]	0.00	0.80	0.68	0.49	0.09	0.00

In **Scenario 2,** a sailing vessel had to avoid collision with a power-driven target on her starboard. As shown in Figure 13, the minimum-time route (marked as a dotted blue line) would result in a possible collision. The collision risk for this minimum-time route is shown in Table 10. The target's domain would be violated after about 210 minutes from the simulation start. Following this, DDV would increase to 0.4 (216 minutes from the start), indicating a considerable collision risk. As opposed to Scenario 1, this time, avoiding collision is easier due to the favourable wind from the north during the first 5 hours. According to the updated route (marked as a solid blue line), the sailing vessel can navigate to starboard (a major change from the least-time route at the start) and change course again once the collision risk no longer exists. DDV is 0 along the route: the passing distance is 2.7 NM (much larger than 0.65 NM of the domain's astern sector). If the target turned to starboard, the passing distance would be even larger. Furthermore, evasive manoeuvres are done at a relatively small cost of only 9 minutes of extra passage time.
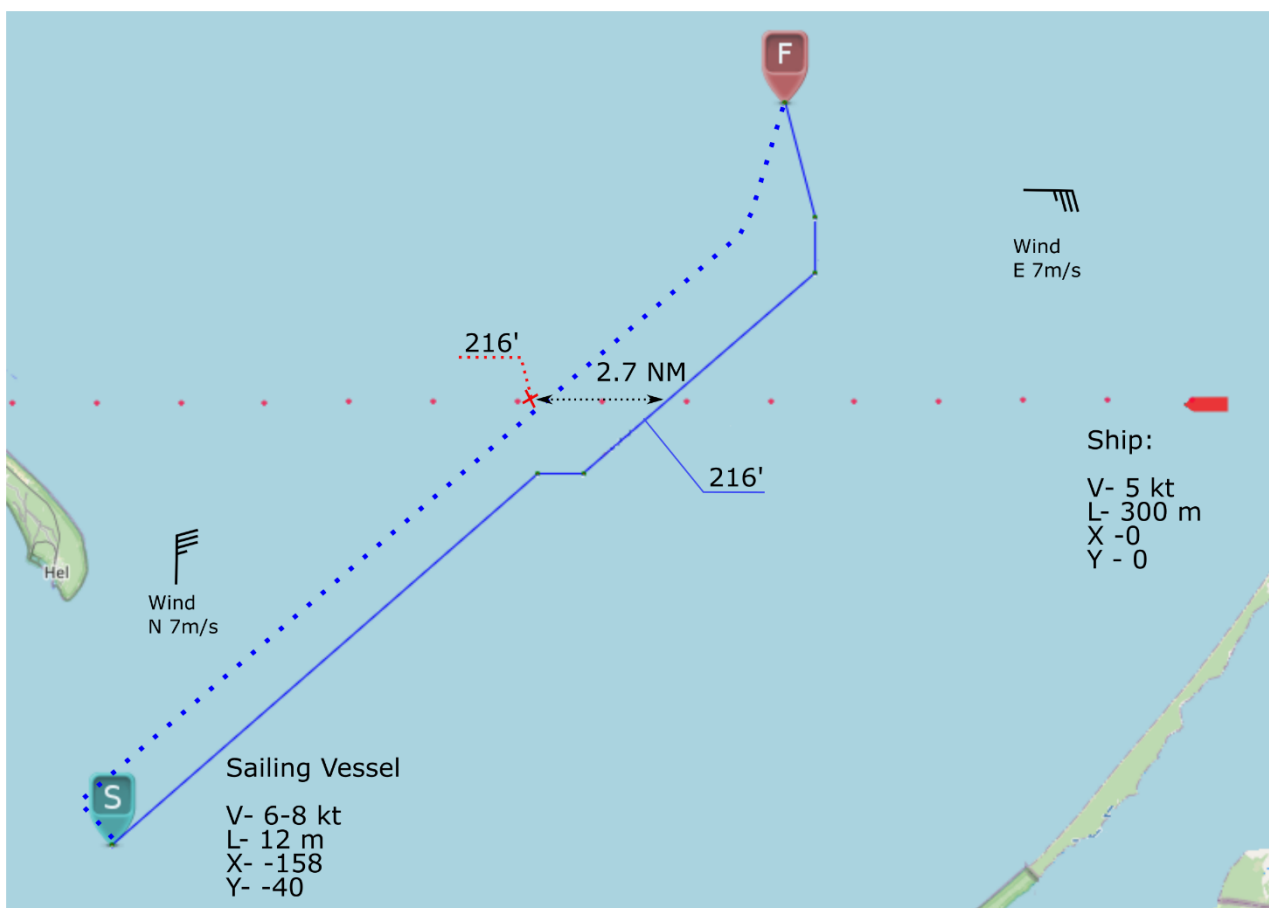

Figure 13. Scenario 2: A sailing vessel avoids collision with a power-driven ship on starboard by passing astern. Least-time route of a sailing vessel is marked as a dotted blue line, collision avoidance route – as a solid blue line and the target's path – as a dotted red line.

Table 10. Collision risk for Scenario 2 (minimum-time route marked as the dotted blue line in Figure 13).

Time [min]	204	210	216	222	226
DDV [/]	0.00	0.10	0.40	0.10	0.00

In **Scenario 3,** a sailing vessel had to overtake a power-driven target. As shown in Figure 14, the minimum-time route (marked as a dotted blue line) could lead to a collision. The collision risk for this minimum-time route is shown in Table 11. The target's domain would be violated about 355 minutes from the simulation start, and DDV would later rise to 1 (376 minutes from the start), which can be interpreted as a large collision risk. A close encounter would last over 25 minutes – longer than for previous scenarios due to the very low relative speed of the two objects. As opposed to Scenario 1 and Scenario 2, this time, the updated route does not cross that of the power-driven target. Instead, the sailing ship tacks to starboard before a risk develops and then sails on a parallel course with a passing distance of 3.5 NM. The target's domain is not violated – DDV remains 0 along the route. The extra cost of evasive manoeuvres is about 6 minutes.
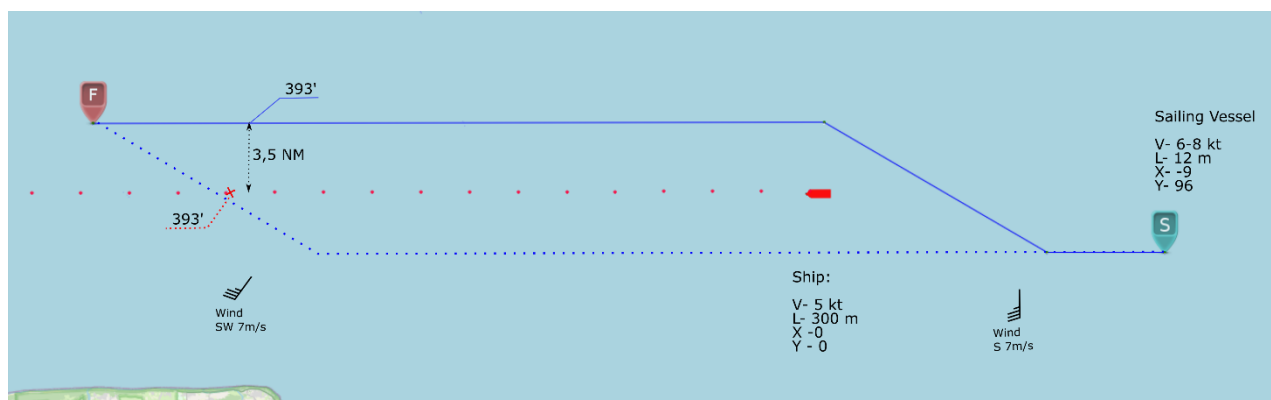

Figure 11. Scenario 3: A sailing vessel avoids collision with a power-driven ship ahead of her. Least-time route of a sailing vessel is marked as a dotted blue line, collision avoidance route – as a solid blue line and the target's path – as a dotted red line.

Table 11. Collision risk for Scenario 3 (minimum-time route marked as the dotted blue line in Figure 14).

Time [min]	350	355	360	366	371	376	382	387	392	397	403
DDV [/]	0.00	0.11	0.41	0.70	0.70	1.00	0.70	0.70	0.41	0.11	0.00

In **Scenario 4,** a sailing vessel had to avoid a head-on collision with a power-driven target ahead of her. As shown in Figure 15, the least-time route (marked as a dotted blue line) would result in a likely incident. The collision risk for this minimum-time route is shown in Table 12. The target's domain would be violated about 240 minutes from the simulation start, and DDV would quickly rise to 0.7, meaning a close-quarters situation. Due to the high relative speed of the two objects, the situation develops quickly: the whole domain violation timespan is below 7 minutes. Again, the proposed method finds a satisfactory solution to this. According to the updated route (marked as a solid blue line), the sailing vessel should tack strongly to her starboard, pass the power-driven target and tack back to port. The passing distance would be over 3.5 NM (compared to the domain's side sector of about 0.65 NM), so DDV would be 0. The evasive manoeuvres would result in only 3 minutes of extra time (about 0.5% of the total passage time).
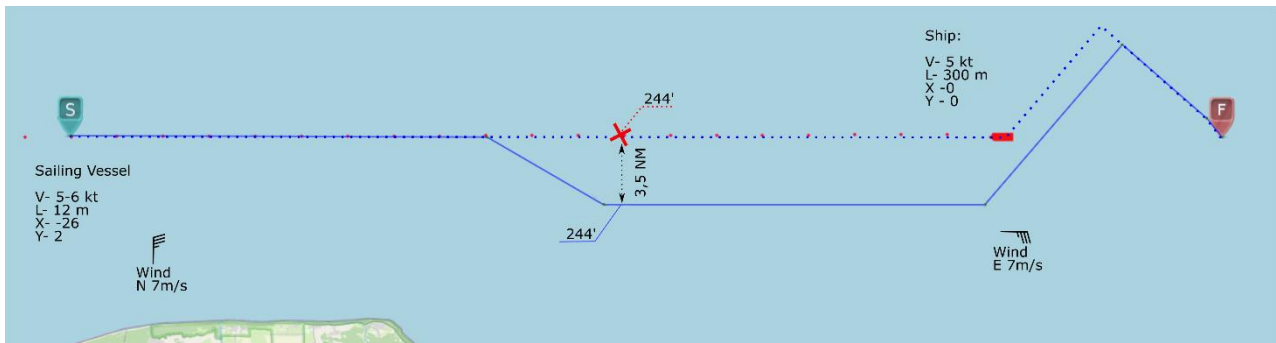
Figure 12. Scenario 4: A sailing vessel avoids a head-on collision with a power-driven ship by tacking to starboard and then back to port. Least-time route of a sailing vessel is marked as a dotted blue line, collision avoidance route – as a solid blue line and the target's path – as a dotted red line.

Table 12. Collision risk for Scenario 4 (minimum-time route marked as the dotted blue line in Figure 15).

6.3 Sensitivity Study and the Impact of Ship Domain Modelling on Computational Time

The proposed method aims to optimize a sailboat's collision-free route, which results in the final route being sensitive to data changes. Practically every significant change in wind speed or direction will result in a change in the optimal route. However, this work studies whether a changed route will remain safe. The sensitivity of a given route's safety is investigated below for Scenario 2 and Scenario 4 from the previous subsection – for crossing and head-on encounters, respectively.

For the route obtained in Scenario 2 (crossing encounter, Figure 13), the sailboat's distances from the target were checked for wind speeds and directions different from the initial input data. The results are in Figure 16. Depending on the wind speed, the sailboat would reach a turning point at different times. DCPA would vary from 7 NM for the wind speed of 7 m/s NNE down to 1.8 NM for the wind speed of 9 m/s NNW. The latter is the bordering value for a slight domain violation (the domain remains non-violated for other cases). Larger domain violations would occur for further increases in wind speed.
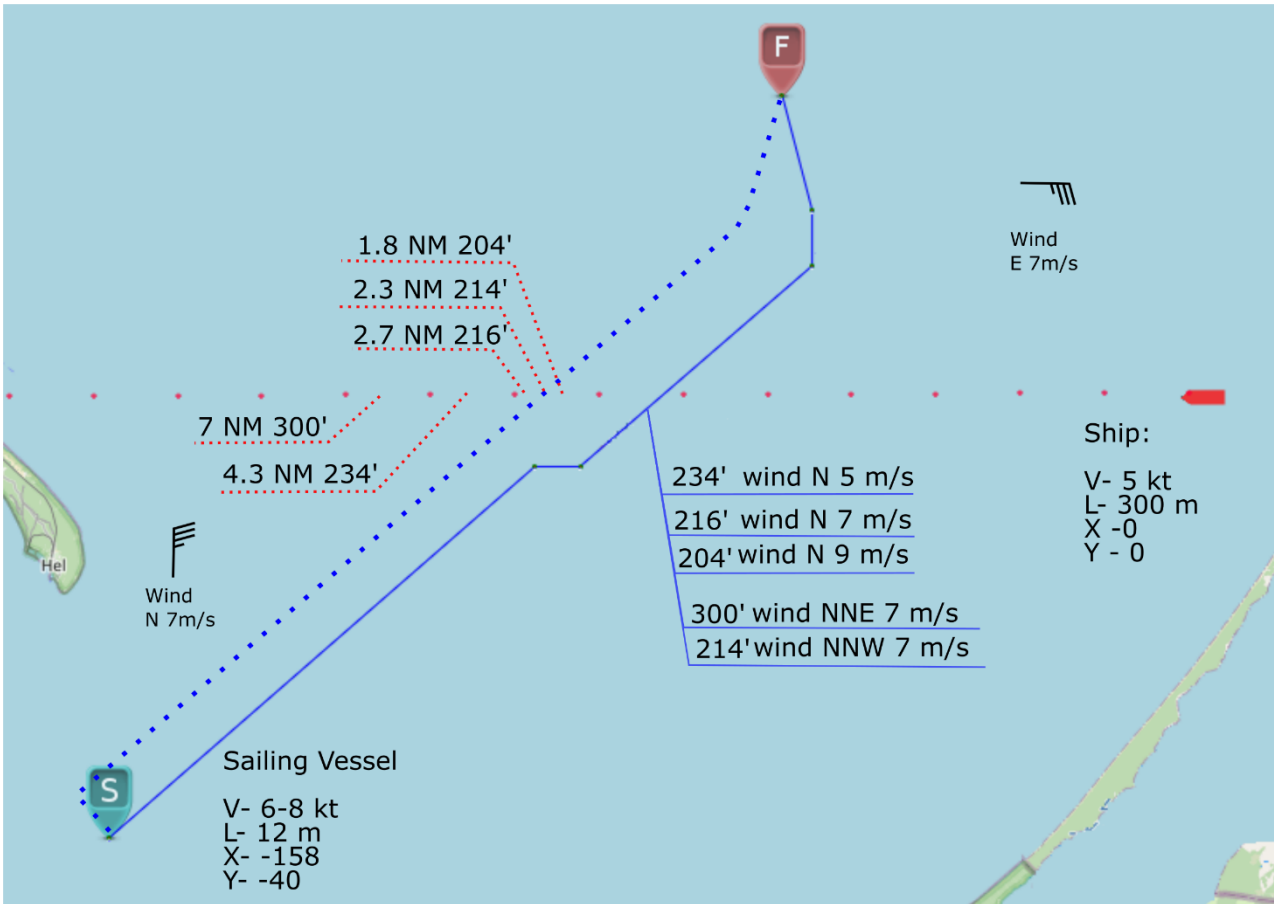
Figure 13. Scenario 2: A sailing vessel avoids a head-on collision with a power-driven ship by tacking to starboard and then back to port. The collision avoidance route is marked as a solid blue line, and the target's path – as a dotted red line. Minimal passing distance for various wind conditions is shown.

In Scenario 4 (a head-on encounter, Figure 15), the sailboat's distances from the target were simulated for different wind speeds and directions. The results are in Figure 17. The distance at which the course is changed would vary from over 14 NM for the wind speed of 9 m/s down to 6 NM for the wind speed of 3 m/s and from 13.5 NM (for NNE instead of N wind direction) down to about 12.5 NM (for NNW wind direction). DCPA does not change and is 3.5 NM regardless of the changes in wind and resulting changes in the own positions. Therefore, the domain remains non-violated for all simulated wind speeds and directions.
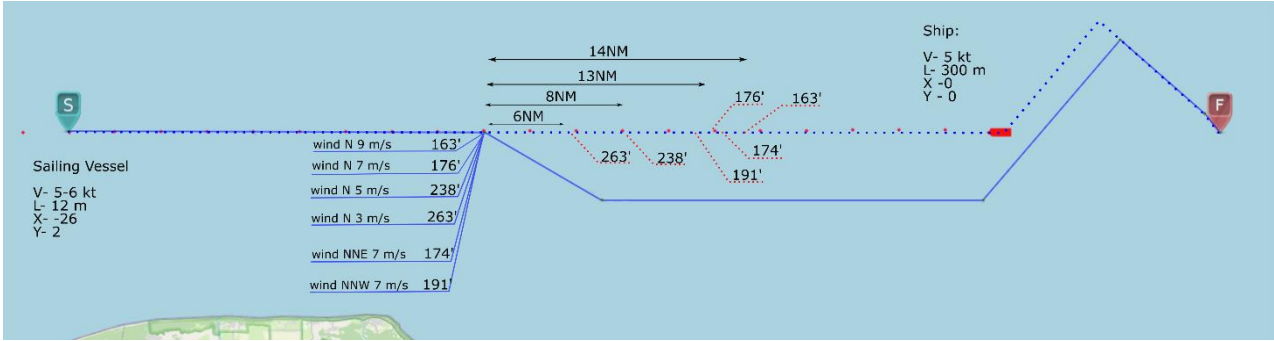

Figure 14. Scenario 4: A sailing vessel avoids a head-on collision with a power-driven ship by tacking to starboard and then back to port. The collision avoidance route is marked as a solid blue line, and the target's path – as a dotted red line. Black arrows mark the distance at which a turn to starboard is made depending on wind conditions.

6.4 The Influence of Weather Forecast Updates on the Determined Route

In this additional scenario (Table 13), the weather changes after 100 minutes. The algorithm for finding the optimal route considers the change in weather conditions as long as appropriate weather forecasts are provided. Two realizations of the scenario are presented here. The first is a route based on two subsequent weather forecasts, while the second is based only on the first forecast. Both routes take into account collision avoidance. As shown in the presented results (Table 13 and Figure 18), sailboats avoided collision with a power-driven ship by passing behind the ship's stern on both routes. However, planning a route based on a single forecast led to a significant error in assessing own speed and thus resulted in determining a path which took longer by more than 3 hours. In comparison, taking into account two subsequent forecasts from the start enabled the method to accurately assess sailing ships and determine a more time-efficient route.

Table 13 Data for the scenario illustrating the influence of weather forecast updates on the determined route.

| Scenario data			
Sailing vessel start position	55.37° N 19.27° E	Distance and bearing at the start	28 NM 155°
Sailing vessel destination position	55.68° N 18.05° E	Sailboat's initial relative position in the target x_s, y_s	66 -69
Target ship start position	55.75° N 18.90° E	$t_{\Delta\alpha}$ – penalty factor for turns, used in Formula (14)	8 s / deg.
Target ship speed and course	15 kt 180°	Wind direction and speed	NW 6 m/s (<100 min) and S 4 m/s (>100 min)
Constant weather conditions are assumed (green line)		New weather forecast taken into account in advance (blue line)	
Total time	688' (+192')	Total time	496'
Number of course changes (one forecast)	2	Number of course changes	3
Potential collision time (for collision avoidance mode turned off)	15'	Potential collision time (for collision avoidance mode turned off)	47'
Distance and bearing at the crossing point (15' from the start)	25 NM, 325°	Distance and bearing at collision time (47' from the start)	17NM, 305°
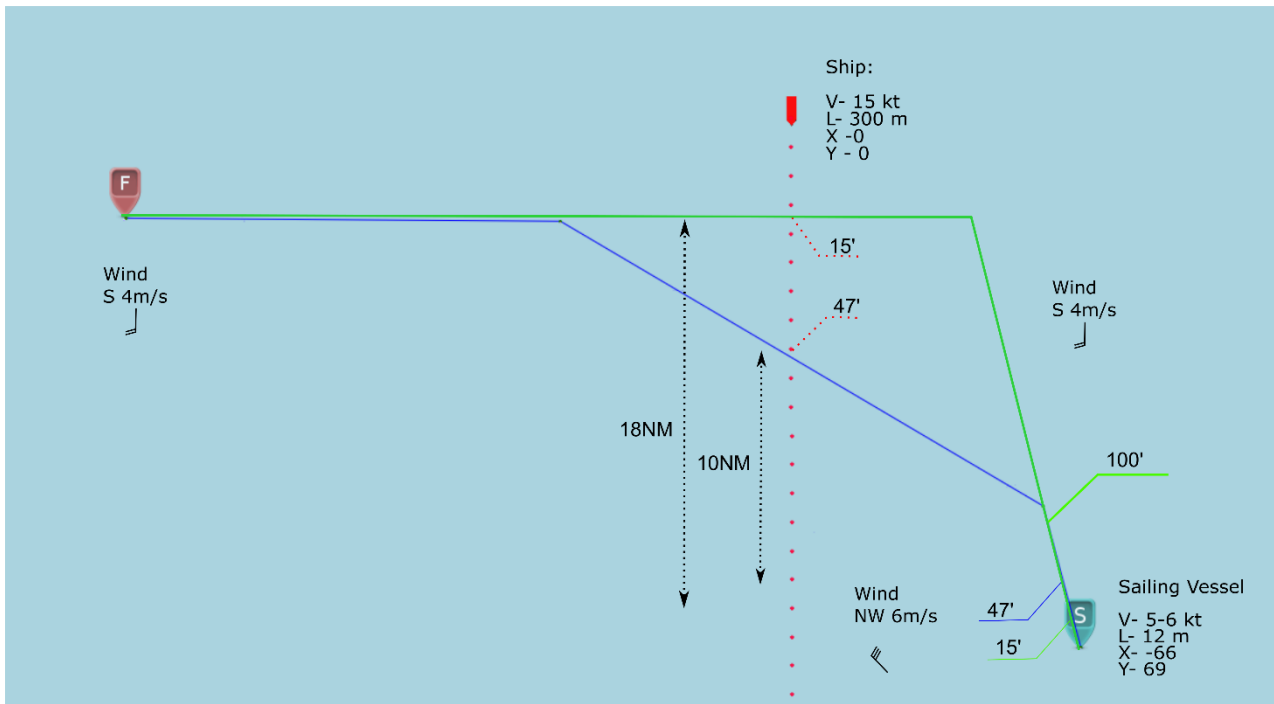
Figure 18. The influence of wind changes on the optimal route. Wind speed and direction: NW 6 m/s <100 min and S 4 m/s >100 min. The route marked with the blue line takes into account the wind change after 100 minutes, while the route marked with the green line does not take into account the change and results in a much longer overall time.

6.5 Risk Monitoring and Route Update

This scenario illustrates risk monitoring and its impact on route updates. Scenario data are based on Scenario 4 from Subsection 6.2 but include additionally an unexpected (and highly unlikely) manoeuvre made by the power-driven ship. The data are in Table 14.

Table 14. Data for the scenario illustrating risk monitoring and its impact on route update

Scenario data			
Sailing vessel start position	55.38° N 17.87° E	Number of course changes (for the updated route)	6
Sailing vessel destination position	55.58° N 17.87° E	Wind speed and direction	N 7 m/s (<400 min) and E 7 m/s (>400 min)
Target ship start position	55.56° N 17.87° E	$t_{\Delta\alpha}$ factor used in Formula (14)	8 s / deg.
Target ship speed and course at the start	15 kt 270°	Target Ship Speed and Course after 209'	15 kt 180°
Potential collision time (without risk monitoring and route update)	265'	Distance and bearing at collision time (for the updated route)	3 NM, 90°

The sailboat's route is planned to avoid collision with a power-driven vessel. As a result, the predicted DDV is zero all along the determined route. It is assumed that the power-driven target will maintain constant speed and course. However, the system still monitors the predicted DDV

parameter when navigating along the route. After 209 minutes from the simulation start, the power-driven target unexpectedly changes course by 90 degrees to port. As soon as the target's new course is detected by the sailboat's AIS, the predicted DDV values are updated (Table 15).

Table 15. Predicted DDV values after the power-driven ship's unexpected turn to port by 90 degrees

Time [min]	237	247	253	256	259	262	265	268	271	274	276
DDV [/]	0.00	0.30	0.57	0.65	0.73	0.81	1.00	0.77	0.54	0.32	0.05

As can be seen, DDV would rise to 0.3 at the 247th minute and reach 1 at the 265th minute, suggesting a significant collision probability. Therefore, the originally planned route is no longer safe and needs to be updated. The route is consequently re-planned for the current data, so the predicted DDV is 0 again. The original route (a dotted blue line) and updated route (a solid blue line) are both shown in Figure 19. For the updated route, the minimal distance between both ships is over 4 NM, and the sailboat passes astern of the power-driven ship.
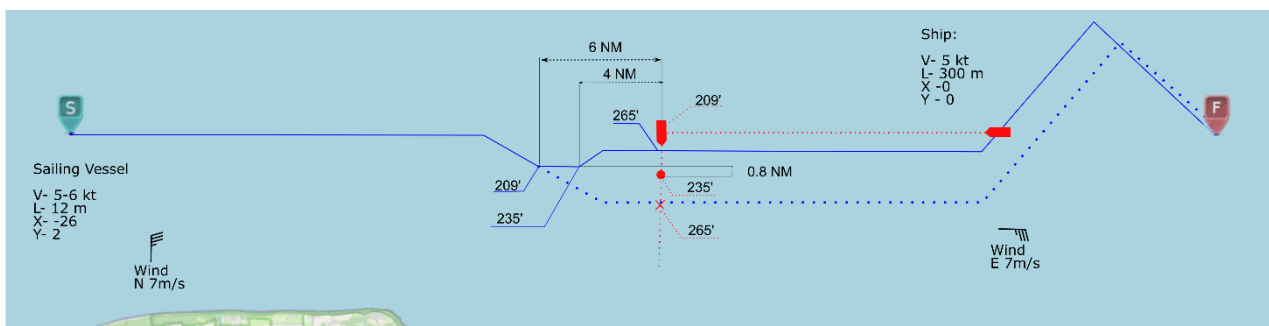

Figure 19. The power-driven ship changes course after 209 minutes. The previously determined sailboat's route (the dotted blue line) is no longer safe (collision at 265' marked with a red cross) and needs to be re-planned (the solid blue line).

Time [min]	239	240	242	243	245	247
DDV [/]	0	0.11	0.70	0.70	0.41	0

7 DISCUSSION OF RESULTS

The discussion of basic and detailed scenarios (data – Subsections 5.2 and 5.3, results – Subsections 6.1 to 6.5) is provided below, followed by a summary of the method's limitations.

7.1 Basic Verification and Detailed Scenarios

As for basic verification, safe solutions were found for all 23 cases. Similarly, the method successfully determined collision-free routes for all four detailed test scenarios (Subsection 6.2). The updated routes avoided violating the target's domains, achieved without a significant increase in the total travel time, even if wind direction was unfavourable. The extra time due to evasive manoeuvres varied from 0.5% to 5% of the total passage time, which can be considered acceptable if we consider that (as opposed to power-driven ships) the increase in time is not associated with increased fuel consumption and emissions.

In terms of the method's sensitivity analysis (results given in Subsection 6.3), the solutions for head-on and crossing remain safe for wind speed or direction largely differing from the initially predicted. However, the overtaking encounter (unlikely in practice) would be more problematic. For wind speeds larger than predicted, the sailboat would approach the target faster and overtake it sooner. For wind speeds much lower than predicted, the sailboat's speed would be lower than that of the target and overtaking would not occur. Unfortunately, there is also a narrow range of wind speeds, which, although significantly lower than predicted, still make it possible for a sailboat to overtake the target. In such a case, the overtaking would take much longer than expected, and the sailboat would not be able to turn to port at the determined waypoint. The route would then have to be updated for the current positions of both ships.

Another related issue is the impact of modelling the target's domain on the method's results and computational time (details in Subsection 6.4). For the presented scenarios, the total computational time can be reduced (on average) by 1% if the 2-step domain violation detection is replaced with a simplified 1-step procedure. However, the above reduction in computational time comes at the cost of increased total navigational time of about 1% on average.

Yet another aspect is the impact of planning a route based on a single (not updated) forecast (results in Subsection 6.5). It may lead to a significant error in assessing own speed and thus determining a much longer path. In comparison, taking into account two subsequent forecasts from the start enables the method to accurately assess sailing ships and determine a more time-efficient route. This confirms the necessity of performing true update-based weather routing instead of relying on single forecasts. Similarly important is the method's risk monitoring feature (Subsection 6.6). Without it, an unexpected turn of a power-driven vessel could greatly increase collision risk and (if overlooked by the sailboat) – lead to an incident.

7.2 Limitations of the Proposed Method

As for now, the practical application of the current version of the method is limited by the following factors.

1. Velocity prediction was based on the assumption that the sailing ship navigates in good visibility, light, stable wind and calm water or small waves. For safety reasons, the method should not be used in other conditions, especially in restricted visibility or harsh weather.
2. It is further assumed that a full sail setup is used and all sails are reasonably trimmed. In the case of other sail setups, the sailboats' speed may differ, which in turn may contribute to reaching some waypoints at different times. In such cases, the navigator should check if the actual trajectory is compliant with the planned route. Alternatively, if another sail setup is to be used by default, a VPP should be re-run, and updated data should be entered.
3. A sailboat's evasive manoeuvres are undertaken here in advance. This is to initiate the own manoeuvre long before the power-driven vessel is obliged to do the same, according to COLREGs. The exceptions are narrow channels and overtaking when manoeuvres can be initiated at a closer distance. However, even then, it should not be too close because a large power-driven vessel can heavily affect waves. Planning or undertaking the manoeuvres in advance is always associated with the risk of the target's course or speed changing and making the planned route irrelevant. If this occurs, the method should be re-run for the current weather conditions and parameters of both ships.
4. Modelling of the thrust of the ship's sail is simplified.
5. The current version of the method does not handle weather forecast-related uncertainties. Thus, the routes may become irrelevant in the extreme case if the actual wind and waves largely differ from the forecasted. In such a case, the navigator should re-run the method for current weather conditions and updated ship positions, courses and speeds.

8 CONCLUSIONS

This paper presents a deterministic method of safe route planning for sailing vessels. The method combines typical weather routing with collision risk monitoring and collision avoidance features. It is based on Dijkstra's algorithm, where edges' weights change in time, and some edges may be temporarily removed due to harsh weather conditions or the presence of other ships. As for the part that handles collision risk, it applies an elliptic domain of a target vessel, where the domain's dimensions depend on the vessel's length. The method was implemented and tested in a series of computer simulations whose examples are provided in the paper. They confirm that collision risk monitoring and collision avoidance can be successfully incorporated into weather routing while keeping the computational time acceptable. If needed, simplified modelling of the ship domain is applied to further reduce the computational time. Furthermore, the detailed results indicate that the method can determine a collision-free route even for larger ship domains and less favourable wind conditions without significantly increasing the total passage time or computational time.

Further work on the method is planned to overcome its limitations described in the previous subsection. Future research directions will include more advanced modelling of sailing vessels' behaviour to loosen weather-related assumptions. Among others, it will address the issue of approximating the thrust of the ship's sail by means of a meta-model and using a larger number of weather forecast parameters, such as currents and significant wave height parameters. This will also make it possible to use additional weather-related dynamic constraints.

ACKNOWLEDGEMENTS

REFERENCES

[1] European Maritime Safety Agency, "Annual Overview of Marine Casualties and Incidents 2019," 2019.

[2] "MAXSURF Design & Analysis Software - Home," 2017.

[3] A. N. (Alfred N. Cockcroft and J. N. F. Lameijer, *A guide to the collision avoidance rules : international regulations for preventing collisions at sea*. Elsevier, 2012.

[4] M. Anninen and P. Kujala, "Influences of variables on ship collision probability in a Bayesian belief network model," *Reliab. Eng. Syst. Saf.*, vol. 102, pp. 27–40, 2012, doi: 10.1016/j.ress.2012.02.008.

[5] P. Kujala, M. Hänninen, T. Arola, and J. Ylitalo, "Analysis of the marine traffic safety in the Gulf of Finland," *Reliab. Eng. Syst. Saf.*, vol. 94, no. 8, pp. 1349–1357, 2009, doi: 10.1016/j.ress.2009.02.028.

[6] M. Zyczkowski, P. Krata, and R. Szłapczyński, "Multi-objective weather routing of sailboats considering wave resistance," *Polish Marit. Res.*, vol. 25, no. 1, 2018, doi: 10.2478/pomr-2018-0001.

[7] M. Zyczkowski and R. Szłapczyński, "Multi-Objective Weather Routing of Sailing Vessels," *Polish Marit. Res.*, vol. 24, no. 4, 2017, doi: 10.1515/pomr-2017-0130.

[8] H. Saoud, M. D. Hua, F. Plumet, and F. Ben Amar, "Routing and course control of an autonomous sailboat," *2015 Eur. Conf. Mob. Robot. ECMR 2015 - Proc.*, pp. 3–8, 2015, doi: 10.1109/ECMR.2015.7324218.

[9] G. Mannarini, D. N. Subramani, P. F. J. Lermusiaux, and N. Pinardi, "Graph-Search and Differential Equations for Time-Optimal Vessel Route Planning in Dynamic Ocean Waves," *IEEE Trans. Intell. Transp. Syst.*, vol. 21, no. 8, pp. 3581–3593, Aug. 2020, doi: 10.1109/TITS.2019.2935614.

[10] F. Tagliaferri, A. B. Philpott, I. M. Viola, and R. G. J. Flay, "On risk attitude and optimal yacht racing tactics," *Ocean Eng.*, vol. 90, pp. 149–154, 2014, doi: 10.1016/j.oceaneng.2014.07.020.

[11] F. Tagliaferri, I. M. Viola, and R. G. J. Flay, "Wind direction forecasting with artificial neural networks and support vector machines," *Ocean Eng.*, vol. 97, pp. 65–73, 2015, doi: 10.1016/j.oceaneng.2014.12.026.

[12] F. Tagliaferri and I. M. Viola, "A real-time strategy-decision program for sailing yacht races," *Ocean Eng.*, vol. 134, no. January 2016, pp. 129–139, 2017, doi: 10.1016/j.oceaneng.2017.02.026.

[13] G. Mannarini, R. Lecci, and G. Coppini, "Introducing sailboats into ship routing system VISIR," *IISA 2015 - 6th Int. Conf. Information, Intell. Syst. Appl.*, no. Cmcc, pp. 1–6, 2016, doi: 10.1109/IISA.2015.7387962.

[14] G. Mannarini and L. Carelli, "VISIR-1.b: Ocean surface gravity waves and currents for energy-efficient navigation," *Geosci. Model Dev.*, vol. 12, no. 8, pp. 3449–3480, 2019, doi: 10.5194/gmd-12-3449-2019.

[15] S. Wei and P. Zhou, "Development of a 3D Dynamic Programming Method for Weather Routing," *Int. J. Mar. Navig. Saf. Sea Transp.*, vol. 6, no. 1, pp. 79–85, 2012.

[16] G. Mannarini, N. Pinardi, G. Coppini, P. Oddo, and A. Iafrati, "VISIR-I: Small vessels - Least-time nautical routes using wave forecasts," *Geosci. Model Dev.*, vol. 9, no. 4, pp. 1597–1625, 2016, doi: 10.5194/gmd-9-1597-2016.

[17] H. Wang, W. Mao, and L. Eriksson, "A Three-Dimensional Dijkstra's algorithm for multi-objective ship voyage optimization," *Ocean Eng.*, vol. 186, no. November 2018, p. 106131, 2019, doi: 10.1016/j.oceaneng.2019.106131.

[18] P. Silveira, A. P. Teixeira, and C. Guedes Soares, "Ais based shipping routes using the dijkstra algorithm," *TransNav*, vol. 13, no. 3, pp. 565–571, 2019, doi: 10.12716/1001.13.03.11.

[19] H. Niu, Y. Lu, A. Savvaris, and A. Tsourdos, "An energy-efficient path planning algorithm for unmanned surface vehicles," *Ocean Eng.*, vol. 161, no. May, pp. 308–321, 2018, doi: 10.1016/j.oceaneng.2018.01.025.

[20] V. Lehtola, J. Montewka, F. Goerlandt, R. Guinness, and M. Lensu, "Finding safe and efficient shipping routes in ice-covered waters: A framework and a model," *Cold Reg. Sci. Technol.*, vol. 165, p. 102795, 2019, doi: https://doi.org/10.1016/j.coldregions.2019.102795.

[21] V. V. Lehtola, J. Montewka, and J. Salokannel, "Sea Captains' Views on Automated Ship Route Optimization in Ice-covered Waters," *J. Navig.*, vol. 73, no. 2, pp. 364–383, 2020, doi: 10.1017/S0373463319000651.

[22]   J. Szlapczynska, "Multi-objective Weather Routing with Customised Criteria and Constraints," *J. Navig.*, vol. 68, no. 02, pp. 338–354, Mar. 2015, doi: 10.1017/S0373463314000691.

[23]   R. Vettor and C. Guedes Soares, "Development of a ship weather routing system," *Ocean Eng.*, vol. 123, pp. 1–14, 2016, doi: 10.1016/j.oceaneng.2016.06.035.

[24]   T. Zvyagina and P. Zvyagin, "A model of multi-objective route optimization for a vessel in drifting ice," *Reliab. Eng. Syst. Saf.*, vol. 218, p. 108147, Feb. 2022, doi: 10.1016/J.RESS.2021.108147.

[25]   P. Krata and J. Szlapczynska, "Ship weather routing optimization with dynamic constraints based on reliable synchronous roll prediction," *Ocean Eng.*, vol. 150, no. December 2017, pp. 124–137, 2018, doi: 10.1016/j.oceaneng.2017.12.049.

[26]   J. Szlapczynska and R. Szlapczynski, "Preference-based evolutionary multi-objective optimization in ship weather routing," *Appl. Soft Comput. J.*, vol. 84, p. 105742, 2019, doi: 10.1016/j.asoc.2019.105742.

[27]   Y.-C. Chang, R.-S. Tseng, G.-Y. Chen, P. C. Chu, and Y.-T. Shen, "Ship Routing Utilizing Strong Ocean Currents," *J. Navig.*, vol. 66, no. 06, pp. 825–835, Nov. 2013, doi: 10.1017/S0373463313000441.

[28]   Y. Huang, L. Chen, P. Chen, R. R. Negenborn, and P. H. A. J. M. van Gelder, "Ship collision avoidance methods: State-of-the-art," *Saf. Sci.*, vol. 121, no. September 2019, pp. 451–473, 2020, doi: 10.1016/j.ssci.2019.09.018.

[29]   M. C. Tsou, "Multi-target collision avoidance route planning under an ECDIS framework," *Ocean Eng.*, vol. 121, pp. 268–278, 2016, doi: 10.1016/j.oceaneng.2016.05.040.

[30]   J. Zhang, D. Zhang, X. Yan, S. Haugen, and C. Guedes Soares, "A distributed anti-collision decision support formulation in multi-ship encounter situations under COLREGs," *Ocean Eng.*, vol. 105, pp. 336–348, 2015, doi: 10.1016/j.oceaneng.2015.06.054.

[31]   A. Lazarowska, "Ship's trajectory planning for collision avoidance at sea based on Ant Colony Optimisation," *J. Navig.*, vol. 68, no. 2, pp. 291–307, 2015, doi: 10.1017/S0373463314000708.

[32]   A. Lazarowska, "A new deterministic approach in a decision support system for ship's trajectory planning," *Expert Syst. Appl.*, vol. 0, pp. 1–10, 2016, doi: 10.1016/j.eswa.2016.11.005.

[33]   A. Lazarowska, "Comparison of Discrete Artificial Potential Field algorithm and Wave-front algorithm for autonomous ship trajectory planning," *IEEE Access*, 2020, doi: 10.1109/ACCESS.2020.3043539.

[34]   R. Szlapczynski and P. Krata, "Determining and visualizing safe motion parameters of a ship navigating in severe weather conditions," *Ocean Eng.*, vol. 158, 2018, doi: 10.1016/j.oceaneng.2018.03.092.

[35]   Y. Huang, L. Chen, and P. H. A. J. M. van Gelder, "Generalized velocity obstacle algorithm for preventing ship collisions at sea," *Ocean Eng.*, vol. 173, no. January, pp. 142–156, 2019, doi: 10.1016/j.oceaneng.2018.12.053.

[36]   A. L. Song, B. Y. Su, C. Z. Dong, D. W. Shen, E. Z. Xiang, and F. P. Mao, "A two-level dynamic obstacle avoidance algorithm for unmanned surface vehicles," *Ocean Eng.*, vol. 170, no. October, pp. 351–360, 2018, doi: 10.1016/j.oceaneng.2018.10.008.

[37]   Y. Wang, X. Yu, X. Liang, and B. Li, "A COLREGs-based obstacle avoidance approach for unmanned surface vehicles," *Ocean Eng.*, vol. 169, no. February, pp. 110–124, 2018, doi: 10.1016/j.oceaneng.2018.09.012.

[38]   P. Silveira, A. P. Teixeira, J. R. Figueira, and C. Guedes Soares, "A multicriteria outranking approach for ship collision risk assessment," *Reliab. Eng. Syst. Saf.*, vol. 214, p. 107789, Oct. 2021, doi: 10.1016/J.RESS.2021.107789.

[39]   A. Zak, "Control of unmanned underwater vehicle as a member of vehicles team performing a given task," *Trans. Marit. Sci.*, vol. 8, no. 1, pp. 18–25, 2019, doi: 10.7225/toms.v08.n01.002.

[40]   A. Zak, "Obstacle Avoidance by Unmanned Underwater Vehicle," *Appl. Mech. Mater.*, vol. 817, pp. 187–196, Jan. 2016, doi: 10.4028/WWW.SCIENTIFIC.NET/AMM.817.187.

[41]   S. Li, J. Liu, and R. R. Negenborn, "Distributed coordination for collision avoidance of multiple ships considering ship maneuverability," *Ocean Eng.*, vol. 181, no. 1178, pp. 212–226, 2019, doi: 10.1016/j.oceaneng.2019.03.054.

[42]   W. Zhang, F. Goerlandt, P. Kujala, and Y. Wang, "An advanced method for detecting possible near miss ship collisions from AIS data," *Ocean Eng.*, vol. 124, pp. 141–156, 2016, doi: 10.1016/j.oceaneng.2016.07.059.

[43]   F. Goerlandt, J. Montewka, W. Zhang, and P. Kujala, "An analysis of ship escort and convoy operations in ice conditions," *Saf. Sci.*, vol. 95, pp. 198–209, Jun. 2017, doi: 10.1016/J.SSCI.2016.01.004.

[44]   S. Xu, E. Kim, S. Haugen, and M. Zhang, "A Bayesian network risk model for predicting ship besetting in ice during convoy operations along the Northern Sea Route," *Reliab. Eng. Syst. Saf.*, vol. 223, p. 108475, Jul. 2022, doi: 10.1016/J.RESS.2022.108475.

[45]   T. Lee, H. Kim, H. Chung, Y. Bang, and H. Myung, "Energy efficient path planning for a marine surface vehicle considering heading angle," *Ocean Eng.*, vol. 107, pp. 118–131, 2015, doi: 10.1016/j.oceaneng.2015.07.030.

[46]   R. Szlapczynski and J. Szlapczynska, "A ship domain-based model of collision risk for near-miss detection and Collision Alert Systems," *Reliab. Eng. Syst. Saf.*, vol. 214, p. 107766, Oct. 2021, doi: 10.1016/J.RESS.2021.107766.

[47]   M. Gil, "A concept of critical safety area applicable for an obstacle-avoidance process for manned and autonomous ships," *Reliab. Eng. Syst. Saf.*, vol. 214, p. 107806, Oct. 2021, doi: 10.1016/J.RESS.2021.107806.

[48]   J. Zhang, Â. P. Teixeira, C. Guedes Soares, and X. Yan, "Quantitative assessment of collision risk influence factors in the Tianjin port,"

Saf. Sci., vol. 110, no. May, pp. 363–371, 2018, doi: 10.1016/j.ssci.2018.05.002.

[49]   F. Goerlandt and P. Kujala, "Traffic simulation based ship collision probability modeling," *Reliab. Eng. Syst. Saf.*, vol. 96, no. 1, pp. 91–107, 2011, doi: 10.1016/j.ress.2010.09.003.

[50]   F. Goerlandt and J. Montewka, "Maritime transportation risk analysis: Review and analysis in light of some foundational issues," *Reliab. Eng. Syst. Saf.*, vol. 138, pp. 115–134, 2015, doi: 10.1016/j.ress.2015.01.025.

[51]   J. Montewka, T. Hinz, P. Kujala, and J. Matusiak, "Probability modelling of vessel collisions," *Reliab. Eng. Syst. Saf.*, vol. 95, no. 5, pp. 573–589, 2010, doi: 10.1016/j.ress.2010.01.009.

[52]   M. Gil, P. Kozioł, K. Wróbel, and J. Montewka, "Know your safety indicator – A determination of merchant vessels Bow Crossing Range based on big data analytics," *Reliab. Eng. Syst. Saf.*, vol. 220, p. 108311, Apr. 2022, doi: 10.1016/J.RESS.2021.108311.

[53]   C. H. Chang, C. Kontovas, Q. Yu, and Z. Yang, "Risk assessment of the operations of maritime autonomous surface ships," *Reliab. Eng. Syst. Saf.*, vol. 207, p. 107324, Mar. 2021, doi: 10.1016/J.RESS.2020.107324.

[54]   M. Zhang, J. Montewka, T. Manderbacka, P. Kujala, and S. Hirdaris, "A Big Data Analytics Method for the Evaluation of Ship - Ship Collision Risk reflecting Hydrometeorological Conditions," *Reliab. Eng. Syst. Saf.*, vol. 213, p. 107674, Sep. 2021, doi: 10.1016/J.RESS.2021.107674.

[55]   J. E. Kerwin, "A Velocity Prediction Program for Ocean Racing Yachts," *Rep 78 - 11 MIT*, 1978.

[56]   J. Gerritsma, J. A. Keuning, and R. Onnink, "The Delft Systematic Yacht Hull Series II Experiments," 1990.

[57]   N. Salvesen, E. Tuck, and O. Faltinsen, "Ship motions and sea loads," *Trans. SNAME*, vol. 78, no. i. pp. 250–287, 1970, doi: citeulike-article-id:10193407.

[58]   R. Szlapczynski and J. Szlapczynska, "A Simulative Comparison of Ship Domains and Their Polygonal Approximations," *TransNav*, vol. 9, no. 1, pp. 135–141, 2015, doi: 10.12716/1001.09.01.17.

[59]   R. Szlapczynski, P. Krata, and J. Szlapczynska, "Ship domain applied to determining distances for collision avoidance manoeuvres in give-way situations," *Ocean Eng.*, vol. 165, 2018, doi: 10.1016/j.oceaneng.2018.07.041.

[60]   R. Szlapczynski and J. Szlapczynska, "An analysis of domain-based ship collision risk parameters," *Ocean Eng.*, vol. 126, 2016, doi: 10.1016/j.oceaneng.2016.08.030.